CHAPTER 2

One-Pot Sequential Knoevenagel Condensation and Palladium-Catalyzed Intramolecular Cross-Dehydrogenative Coupling: Access to Imidazopyridine-fused Indoles

Chapter 2

2.1 INTRODUCTION

The construction of heterocyclic complex molecules with high efficiency in respect of minimization of synthetic steps and high complexity is always a challenging task for the synthetic chemist.[1-2] Hence, the development of a simple and convenient approach for the synthesis of heterocyclic compounds is highly desirable. In this aspect, tandem, and multi-component reactions have proven to be more powerful strategy in organic synthesis. The benefits of these reactions are atom economical, high yielding in one-pot and environmentally benign over the classic methods. Also, it minimizes the step of separation and purification during reactions.[3-6] Several synthetic transformations have been done in a one-step and ultimately reduces the synthetic steps, avoid reactive and toxic solvents as well as its cost.[7]

2.1.1 Tandem Reaction

The term tandem is defined as a chemical process, which consists of at least two consecutive reactions in one pot and each subsequent reactions occur only in virtue of the chemical functionality formed in the previous step. These types of reactions are also known as cascade or domino or sequential reactions. These types of reactions often proceed *via* a highly reactive intermediate. Also, in these reactions, the substrate undergoes the sequential transformation into two or more mechanical distinct processes. A simple representation of the tandem process is shown in **Figure 2.1.** The designed targeted molecule could be achieved in a single step using tandem protocol while by traditional methods it has to pass through an intermediate stage.

The major advantages of the tandem reactions are as follows

a) It does not involve work up, isolation of intermediate and hence reduces the labor and time.
b) It build a large number of complexity in a single step.
c) It reduces waste generation.

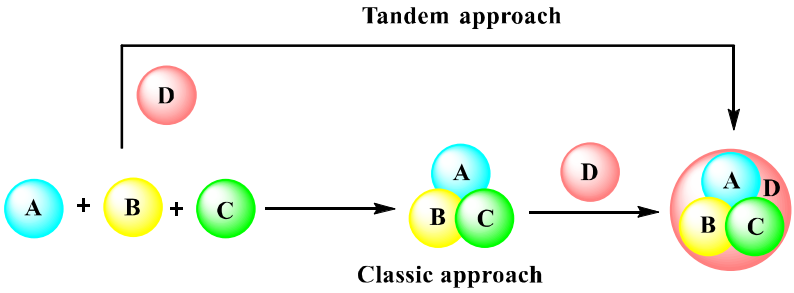

Figure 2.1 Schematic representation of tandem reactions

2.1.2 Cross-Dehydrogenative Coupling Reactions

Cross-dehydrogenative coupling (CDC) reactions are another class of organic chemistry that has provided an efficient and powerful strategy for the synthesis of biheteroaryl compounds.[8] The coupling between two hetero(arene) C–H bonds with the evolution of "H_2" gas termed as cross-dehydrogenative coupling reactions. The removal of H_2 gas is not thermodynamically favorable, so it requires some oxidant and therefore it is also called oxidative C–H/C–H coupling.[9] Transition metal-catalyzed C–H cross-coupling reaction is also an important methodology used in the construction of natural products, pharmaceuticals, and organic functional materials.[10]

This approach provides significant advantages over traditional cross-coupling reactions as well as C–H activation.[11] From atom and step economy standpoints, the oxidative C–H/C–H coupling represents a very attractive, sustainable, and ideal approach towards the synthesis of biheteroaryl compounds.[12] On the basis of the construction of biheteroaryl compounds, the cross-dehydrogenative coupling is divided into two types: Intermolecular and Intramolecular CDC. In recent years intermolecular cross-dehyrogenative coupling reactions have been exclusively studied.[13-14] However, intramolecular CDC reactions are relatively less explored as pre-installation of directing group is difficult for thise reactions.

A brief overview of the recent development in this intramolecular CDC reactions for synthesis of polyheterocyclic compound is presented below.

2.1.3 Intramolecular Cross-Dehydrogenative Coupling

The intramolecular cross-coupling is one of the efficient and strightforward methods to access the polycyclic compounds, especially tricyclic bi(hetero)aryl moieties **(Figure 2.2)**. Despite their importance, very few synthetic strategies are available to achieve these fused frameworks.

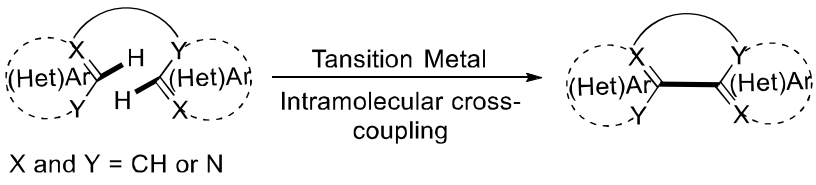

Figure 2.2 Ring closure reaction *via* intramolecular oxidative C–H/C–H coupling

Fagnou group reported the palladium-catalyzed intramolecular oxidative coupling reaction of biaryl compounds **(1)** for the synthesis of carbazoles and dibenzofurans **(2) (Scheme 2.1a).**[15] For this transformation, PivOH (Pivalic acid) was the better solvent than AcOH, leading to higher yield and better selectivity. In addition, the derived protocol afforded the naturally occurring carbazole products, such as Murrayafoline A, Mukonine, and Clausenine. Subsequently, Menéndez and co-workers employed microwave-assisted synthesis of carbazoles *via* palladium-catalyzed double C–H activation of diaryl amines **(1) (Scheme 2.1b).**[16]

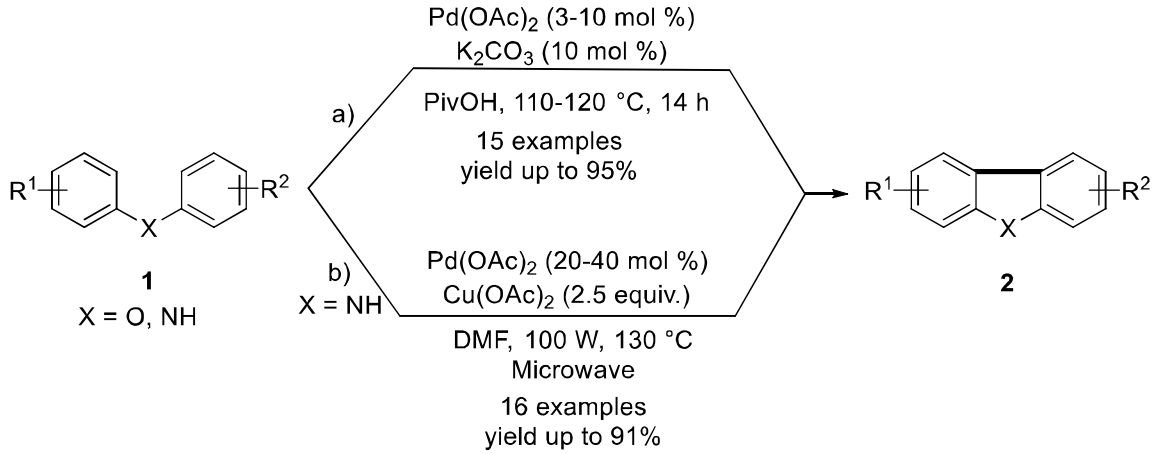

Scheme 2.1 Palladium-catalyzed intramolecular oxidative biaryl synthesis

Chenge *et al*. described palladium-catalyzed oxidative cyclization of biaryl ketones **(3)** for the effective synthesis of fluorenones **(4) (Scheme 2.2).**[17] The intramolecular cyclization procced *via* carbonyl-assisted *ortho* C H activation. Interestingly, in this transformations ketone group acted as a weak directing group. The fluorenones were obtained in good to excellent yields.

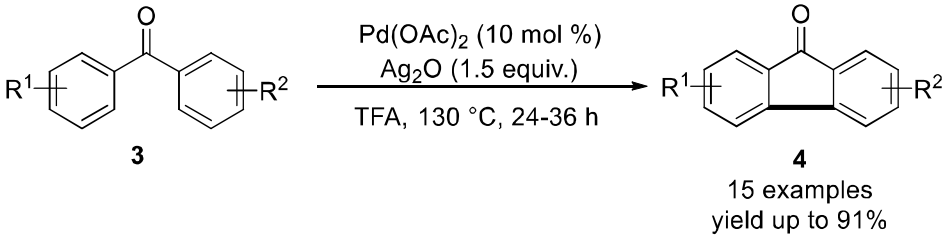

Scheme 2.2 Synthesis of fluorenones *via* Pd-catalyzed oxidative cyclization

Laha and colleagues disclosed the synthesis of annulated biaryl sultams **(6)** through palladium-catalyzed intramolecular oxidative coupling (IOC) involving double C(sp^2)–H in sulfonanilides

(5) (Scheme 2.3a).[18] The free NH group that is susceptible to functionalization at nitrogen. The present protocol was also explored for the synthesis of a seven-membered ring, analogous biaryl sultones, and phenanthridinones. The same group reported palladium-catalyzed biaryl **(8)** formation by intramolecular double C(sp^2)-H functionalization **(Scheme 2.3b)**. The *N*-aryl sulphonyl indoles **(7)** provides an atom-economical green approach for the synthesis of heterobiaryl sultam **(8)**.[19] The described methodology was further demonstrated for the synthesis of *N*-benzyl- or *N*-benzoylindoles. Interestingly, *N*-aryl sulfonyl heterocycles underwent novel ring opening with amines under mild reaction conditions to afford the heterobiaryl sultams in moderate to good yields. In 2018, Laha and co-workers described the synthesis of fused biaryl sulfones *via* palladium-catalyzed oxidative annulation (**Scheme 2.3c)**.[31] The biaryl and heterobiaryl sulfones **(9)** underwent intramolecular oxidative cyclization in the presence of $Pd(OAc)_2$ to afford fused biheteroaryl sulfones **(10)**. The developed method was further extended for the synthesis of fused polycyclic fluorenes, which were used to design single fluorene molecule-based organic emitters.

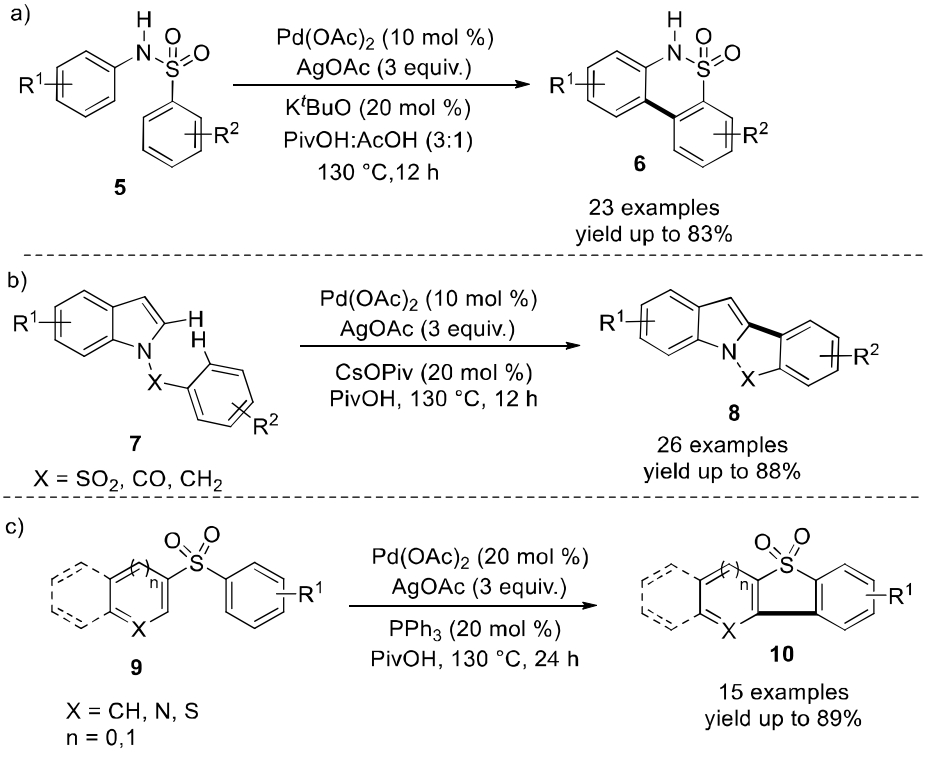

Scheme 2.3 Pd-catalyzed intramolecular oxidative cyclization for the synthesis of fused heterobiaryl sulfones, sulfonamides and *N*-benzoyl- or *N*-benzylindoles

Ackermann group achieved the synthesis of annulated phenanthrenes *via* sequential two distinct C–H bond functionalization reactions **(Scheme 2.4)**.[20] The 1,2,3-triazole **(11)** underwent palladium-catalyzed intramolecular dehydrogenative direct arylation to afford heteroannulated phenanthrenes **(12)** under ambient conditions. This method demonstrated a modular synthesis of π-conjugated heteroannulated phenanthrenes.

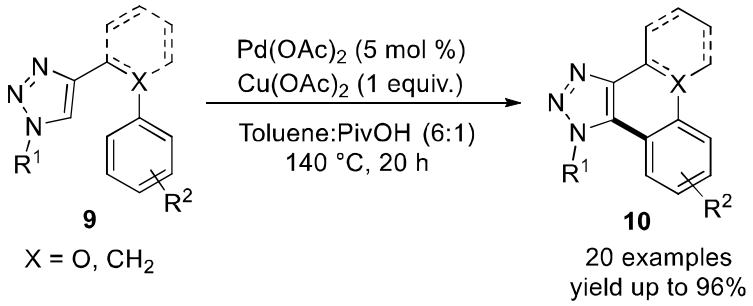

Scheme 2.4 Pd-catalyzed synthesis of annulated phenanthrenes

Bao and co-workers accessed double C(sp^2)–H bond activation between C_2-position of imidazole or benzimidazole and arenes **(11)** *via* palladium-catalyzed intramolecular oxidative C–C bond formation **(Scheme 2.5a)**.[21] The strategy provides an efficient and concise route to the synthesis of imidazole- or benzimidazole-fused isoquinoline heteroaromatic compounds **(12)**. Similarly, Kambe and co-workers reported rhodium(III)-catalyzed intramolecular double bond C–H activation for the synthesis of imidazo and benzimidazo[2,1-*a*]isoquinoline derivatives **(12) (Scheme 2.5b)**.[22]

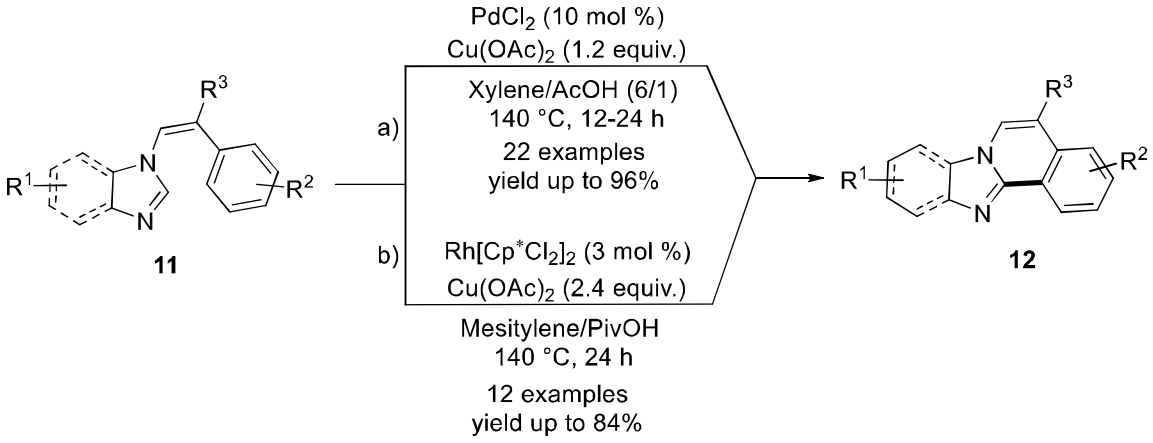

Scheme 2.5 Palladium and rhodium(III)-catalyzed synthesis of imidazo and benzimidazo[2,1-*a*]isoquinoline derivatives

Kanai and Kuninobu groups described palladium-catalyzed intramolecular dehydrogenative coupling for the synthesis of heteroatom-containing ladder-type π-conjugated compounds **(Scheme 2.6)**.[23] The synthesis of ladder-type π-conjugated molecules **(14** and **16)** has been reported from *ortho* phenylene-bridged biaryl compounds **(13)** and heteroatom- or carbonyl-bridged biaryl compounds **(15)** respectively. The efficiency of the described method has been proved by one step synthesis of desired products in moderate to good yields. The synthetic potential of the protocol demonstrated by the gram scale experiment to furnish the annulated product in good yield.

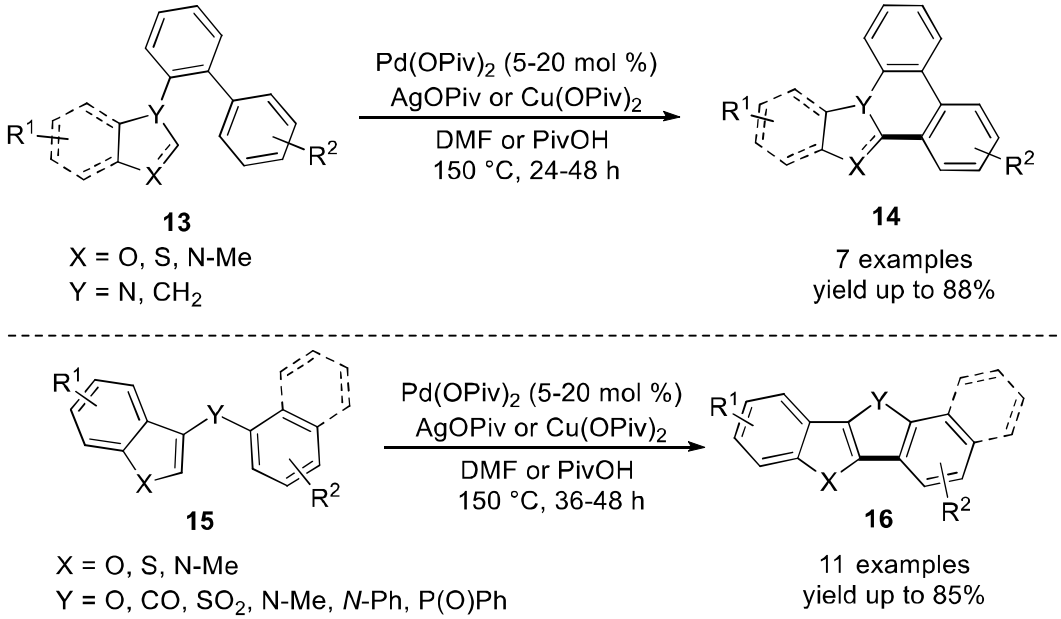

Scheme 2.6 Pd-catalyzed oxidative coupling for ladder-type π-conjugated compounds

Greaney group synthesized medium-ring biaryl compounds through intramolecular oxidative C–C coupling **(Scheme 2.7).**[24] Reactions proceed *via* palladium-catalyzed oxidative coupling of indole with (hetero)arenes **(17** and **19)** to form annulated seven-membered rings **(18** and **20).** The synthesized medium-ring compounds showed versatile applications in medicinal chemistry. The reaction display the large functional groups tolerance and broad substrate scope with good regioselectivity for the synthesis of annulated heterocycles in 43-95% yields.

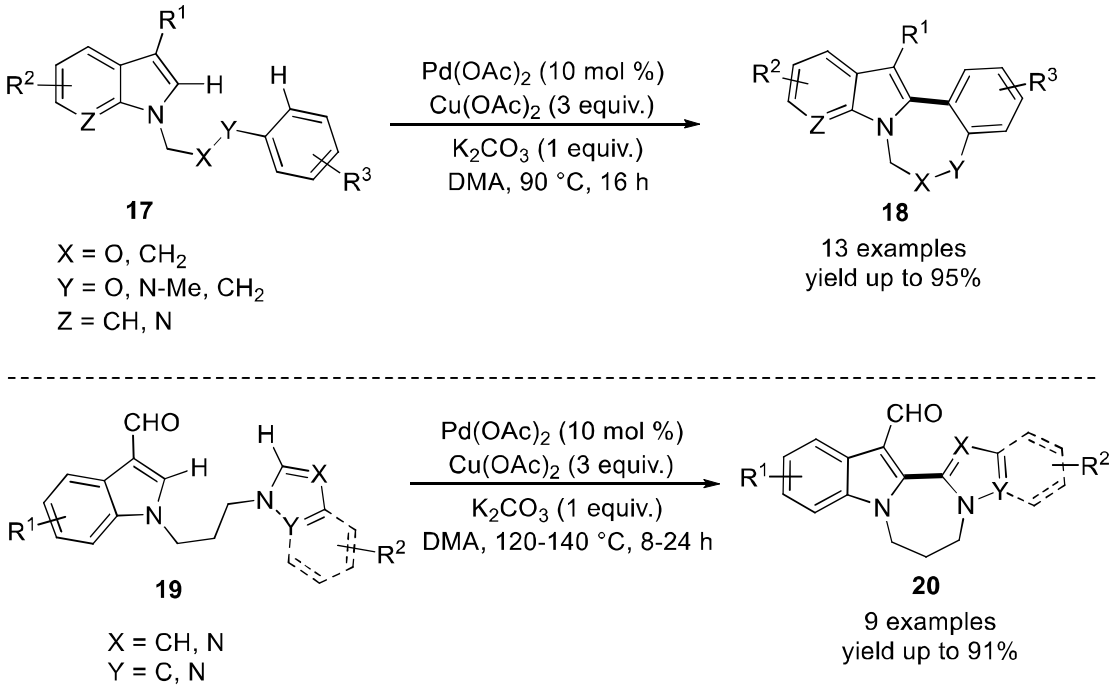

Scheme 2.7 Pd-catalyzed intramolecular oxidative coupling for the synthesis of medium-ring biaryl molecules

Singh and co-workers developed palladium and copper-catalyzed four different protocols for the synthesis of polycyclic heteroarenes. Firstly, the *N*-substituted pyrrole-azoles **(21)** underwent palladium-catalyzed intramolecular oxidative and regioselective C–H/C–H coupling to afford polyheterocyclicarenes **(22) (Scheme 2.8a)**.[25] Selectively C-5 position of pyrrole undergoes C–H activation in the presence of an equally reactive C-2 position**.** Likely, the synthesis of polyheteroarenes **(22)** *via* palladium-catalyzed intramolecular annulation has been reported by using pyrrolylalkyl-1*H*-azoles **(21) (Scheme 2.8b)**.[26] This approach involving dual C(sp^2)–H bond functionalization gave direct access to the six- and seven-membered heteroaryl rings. Subsequently, the synthesis of polycyclic heteroarenes **(22)** has been achieved using copper-catalyzed ligand-assisted intramolecular cross-dehydrogenative coupling between indole-2 and imidazole-2 moieties **(21) (Scheme 2.8c)**.[27] Recently, the copper-catalyzed ligand-free method was reported for the synthesis of pyrrole-annulated heterocycles **(22)** using 3-substituted and 3,4-disubstituted pyrrole–azole systems **(21) (Scheme 2.8d)**.[28] In this case, the C–H bond of the C2 position of pyrrole was site selectively activated over the C5 C–H bond, to get six- and seven-membered annulated pyrrole products.

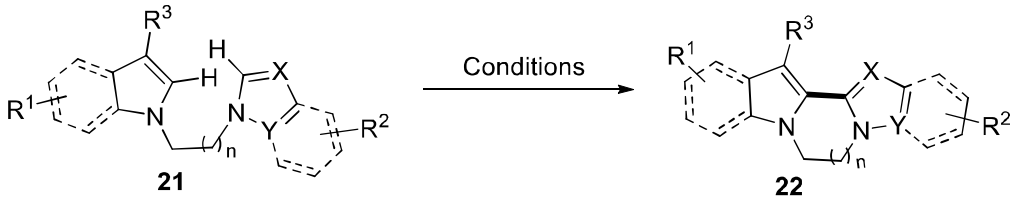

21

X = CH, N; Y = C, N; n = 1, 2

22

No.	Conditions	Examples	Yield
a)	$Pd(OAc)_2$ (10 mol %), Ag_2CO_3 (2 equiv.) 2,6-Luitidine (0.2 equiv.), NMP:DMA (9:1), 130 °C	26	up to 64%
b)	$Pd(OAc)_2$ (10 mol %), AgOAc (2 equiv.) AcOH (5 equiv.), DMF 120 °C	15	up to 83%
c)	$Cu(OAc)_2$ (1 equiv.), 1,10-Phenanthroline (2 equiv.), Ag_2CO_3, K2CO3, Xylene, 140 °C, 12 h	13	up to 84%
d)	$Cu(OAc)_2$ (2 equiv.), Ag_2CO_3 (1 equiv.), NMO K_2CO_3, TBAB, Xylene, 150 °C, 36 h	15	up to 88%

Scheme 2.8 Palladium and copper-catalyzed oxidative annulation for the synthesis of polyheteroarenes

Favi *et al*. discovered the synthesis of polycyclic nitrogen heterocycles *via* the palladium-catalyzed intramolecular oxidative cross-dehydrogenative coupling (**Scheme 2.9)**.[29] The intramolecular oxidative annulation of different C3,*N*-linked indoles and, azoles **(23)** gaves direct access to polycyclic indole scaffolds **(24)**. The methodology acheived for the synthesis of indole-derived natural products and medicinally relevant polycyclic fused compounds.

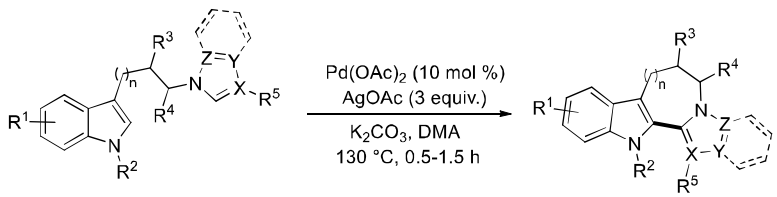

23

X,Y,Z = C, CH or N
n = 0, 1

24

17 examples
yield up to 96%

Scheme 2.9 Synthesis of polycyclic heteroarene *via* Pd-catalyzed intramolecular dual C–H functionalization

Wang group developed a palladium-catalyzed intramolecular oxidative cross-coupling for the synthesis of fused *N*-heterocyclic compounds **(Scheme 2.10).**[30] The tertiary enamides with arenes **(25)** underwent intramolecular arylation to furnish seven-membered ring containing 7,8-dihydro-5*H*-benzo[4,5]azepino[2,1-*a*]isoindol-5-one scaffold **(26).** The developed protocol was used for the synthesis of aporhoeadane alkaloids such as palmanine, lennoxamine, and chilenamine.

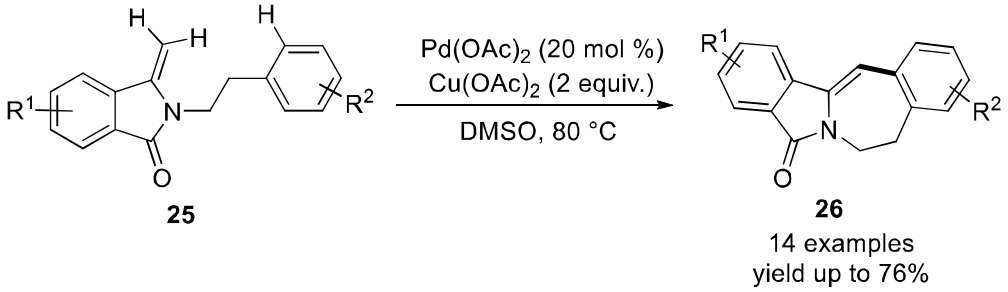

Scheme 2.10 Synthesis of fused *N*-heteroarene *via* Pd-catalyzed intramolecular dehydrogentive coupling

Xu *et al.* disclosed the base-free palladium-catalyzed intramolecular oxidative cross-coupling reaction of 2-aryloxy substituted chromen-4-ones **(29)** reacted intramolecularly to afford the variety of coumaronochromones **(30)** in moderate to good yields **(Scheme 2.13)**.[32] The broad substrate scope, high atom economy and efficiency, good functional tolerance, and non-toxic reagent are the silent features of this methods.

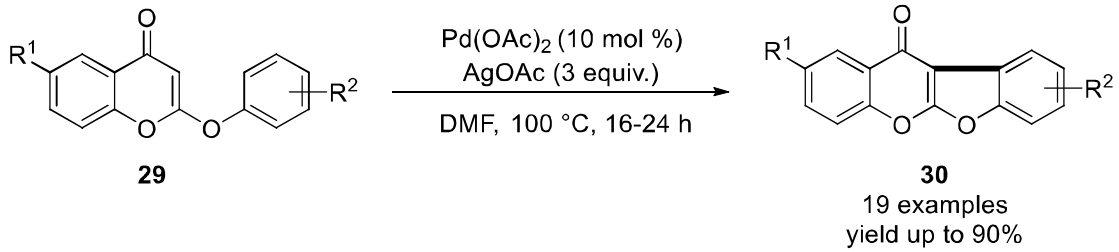

Scheme 2.11 Pd-catalyzed intramolecular cyclization of 2-aryloxy substituted chromen-4-ones

Pal and co-workers demonstrated the synthesis of benzoimidazo[1,2-*a*]isoxazolo[4,3-*c*]quinoline derivatives **(32)** *via* palladium-catalyzed intramolecular dual C–H functionalization protocol **(Scheme 2.12)**.[33] The developed strategy worked well under base-free, co-catalyst-free, and metallic oxidant-free conditions using molecular oxygen as the sole oxidant. Moreover, the described protocol portrayed some significant features such as broad substrate scope, wide

functional group compatibility for the construction of fluorescence active compounds with high quantum yields. The synthetic utility further explored towards the synthesis of pyridine, pyrimidine, pyrazole fused heteropolycyclic compounds through Fe-catalyzed reductive isoxazole ring cleavage.

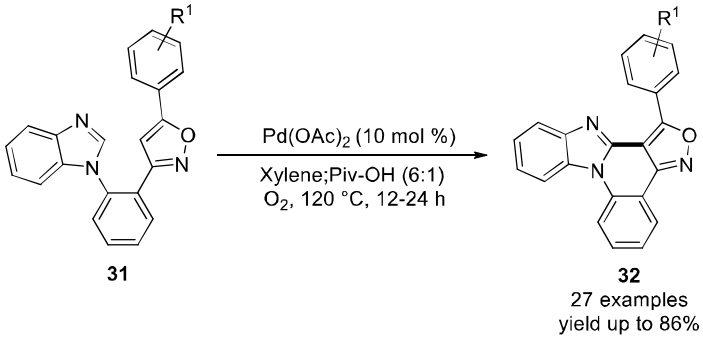

Scheme 2.12 Palladium-catalyzed intramolecular dual C H functionalization for the synthesis of benzoimidazo[1,2-*a*]isoxazolo[4,3-*c*]quinoline derivatives

As evident from literature reports, aza-fused heterocyclic compounds with high molecular complexity can be easily constructed by employing transition metal-catalyzed intramolecular cross-dehydrogenative coupling reaction in tandem fashion. As a part of our continued interest in the synthesis of a new assembly of *N*-fused polyheterocyclic compounds by employing cross-dehydrogenative coupling. In this chapter, we wish to disclose the Pd(II)-catalyzed intramolecular cross-dehydrogenative coupling reaction for the synthesis of imidazopyridine-fused indoles through Knoevenagel condensation between active methylene azoles **(34)** and *N*-substituted-1*H*-indole-2-carbaldehyde **(37)** or *N*-substituted-1*H*-indole-3-carbaldehyde **(33) (Scheme 2.13)**.

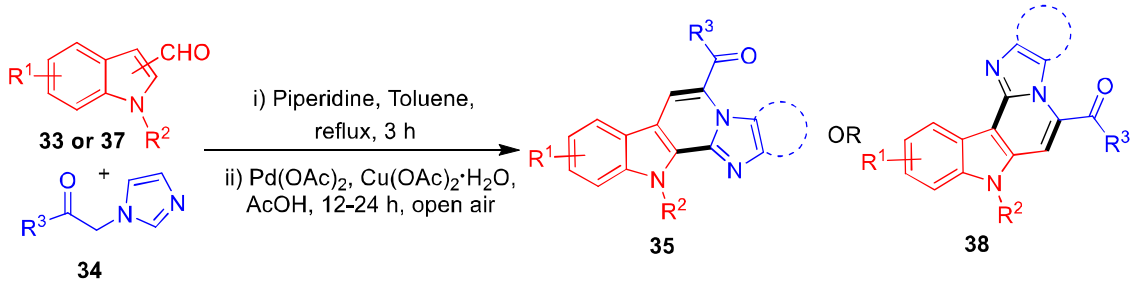

Scheme 2.13 Synthesis of azole annulated indoles *via* Pd-catalyzed intramolecular cross-dehydrogenative coupling

2.2 RESULTS AND DISCUSSION

To evaluate the feasibility of our proposed synthetic pathway, initially we examined the model reaction between 2-(1*H*-imidazol-1-yl)-1-phenylethan-1-one (**34a**) and 1-methyl-1*H*-indole-3-carboxaldehyde (**33a**) in presence of piperidine as a base, $Pd(OAc)_2$ as catalyst, $Cu(OAc)_2 \cdot H_2O$ as oxidant and AcOH as an additive in toluene at 120 °C for 30 h. To our satisfaction, the desired product, 11-methyl-11*H*-imidazo[1',2':1,2]pyrido[3,4-*b*]indol-5-yl)(phenyl)methanone (**35aa**) was obtained with 39% yield along with Knoevenagel condensation product (**36aa)** in 30% yield (**Table 2.2**, entry 1).

The structures of both compounds **35aa** and **36aa** were ascertained by ^{1}H NMR, ^{13}C{^{1}H} NMR, IR and mass spectrometry analysis. In the ^{1}H NMR of **35aa**, two singlets appeared at 8.09 and 4.59 ppm for C6-proton and *N*-methyl proton, respectively (**Figure 2.3**). The carbonyl carbon peak at 189.8 ppm in the ^{13}C NMR spectrum along with other carbon peaks (**Figure 2.4**). The presence of peak at *m/z* 326.1305 in HRMS corresponding to molecular formula $C_{21}H_{16}N_3O$ $[M + H]^+$ ion confirmed the structure of **35aa** (**Figure 2.5**).

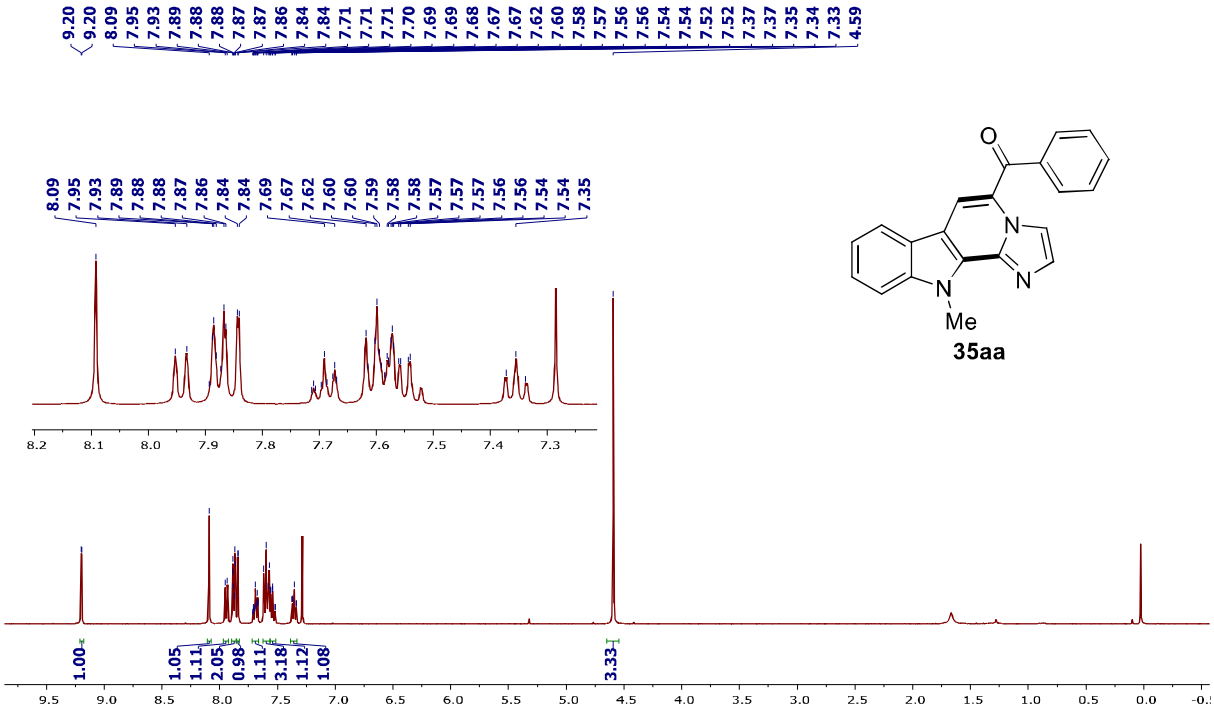

Figure 2.3 ^{1}H NMR spectrum of 11-methyl-11*H*-imidazo[1',2':1,2]pyrido[3,4-*b*]indol-5-yl)(phenyl)methanone **(35aa)** in $CDCl_3$

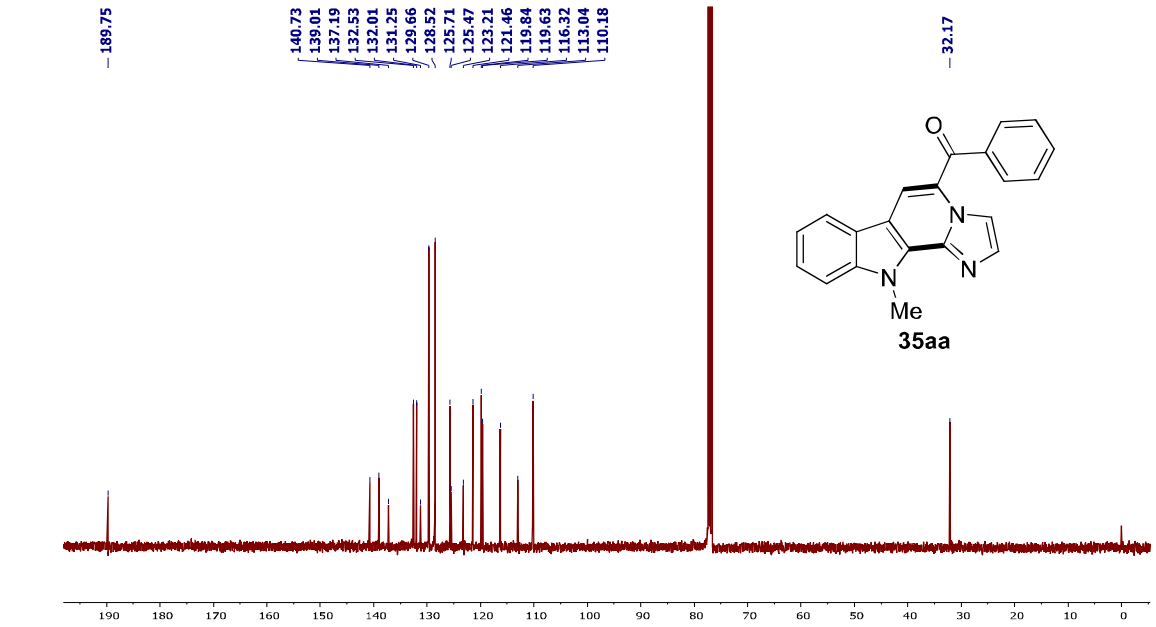

Figure 2.4 $^{13}C\{^{1}H\}$ NMR spectrum of 11-methyl-11*H*-imidazo[1',2':1,2]pyrido[3,4-*b*]indol-5-yl)(phenyl)methanone **(35aa)** in $CDCl_3$

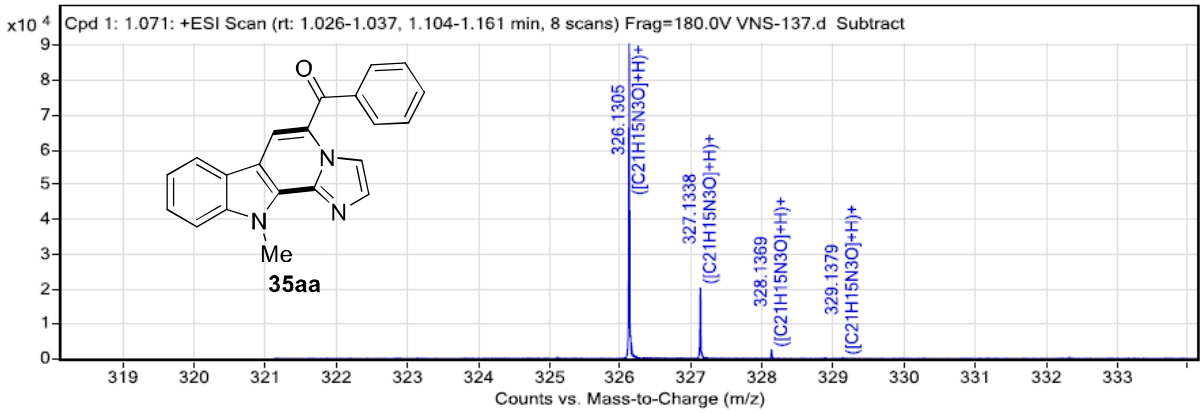

Figure 2.5 LC-HRMS of 11-methyl-11*H*-imidazo[1',2':1,2]pyrido[3,4-*b*]indol-5-yl)(phenyl)methanone **(35aa)**

Similarly, in the ^{1}H NMR of **36aa**, a singlet appeared at δ 8.09 ppm for C3-proton and another singlet at δ 6.99 ppm for C2-proton of indole along with other aromatic and aliphatic protons (**Figure 2.6**). The peaks for carbonyl carbon and *N*-methyl carbon was observed at 191.2 and 33.7 ppm, respectively in the ^{13}C NMR spectrum (**Figure 2.7**). Finally, appearance of a peak at *m/z* 328.1444 in the HRMS spectrum corresponding to molecular ion $C_{21}H_{18}N_3O$ $[M + H]^+$ confirmed the structure of **36aa** (**Figure 2.8**). Interestingly, the structure of **36aa** was also confirmed by X-

ray diffraction analysis (CCDC No. 1821644) (**Figure 2.9**). The **36aa** crystallized in monoclinic crystal system with $P2_1$ space group. The indole and imidazole groups are *cis* to each other around C9=C9 (1.353(3) Å) double bond. The torsional angle between indole ring and olefin group C10-C9-C7-C8 = 5.93° and between the olefin group and imidazole ring C9-C10-N2-C11 = 72.99°, forcing the imidazole ring slightly perpendicular to the indole ring. In the compound 3ha, all the four fused rings are almost planar along with the two carbons of two carbonyl groups, however the phenyl group substitution forming torsional angle of C11-C18-C19-C20 = 47.26°.

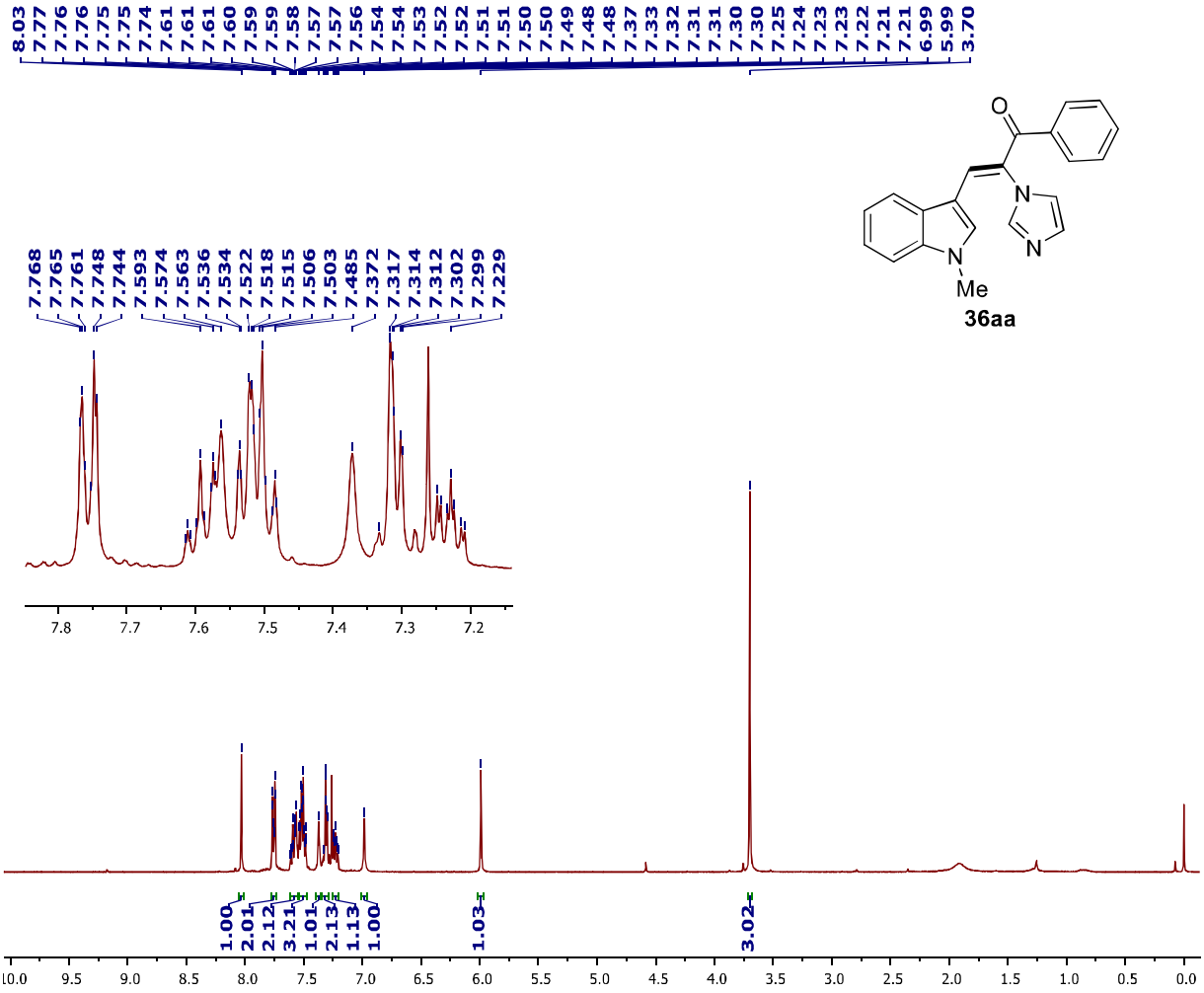

Figure 2.6 ^{1}H NMR spectrum of 2-(1*H*-Imidazol-1-yl)-3-(1-methyl-1*H*-indol-3-yl)-1-phenylprop-2-en-1-one **(36aa)** in $CDCl_3$

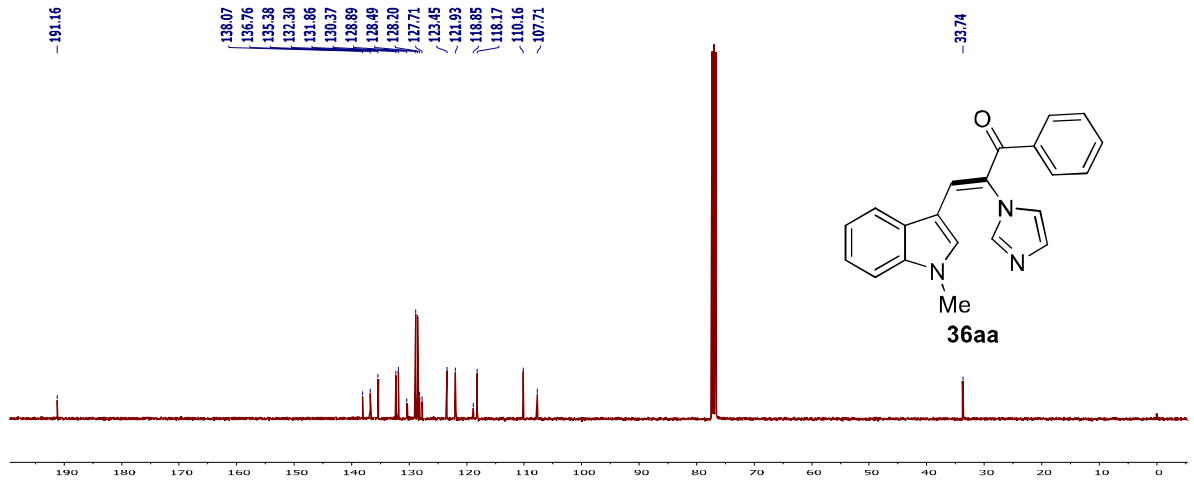

Figure 2.7 ^{13}C NMR spectrum of **36aa** in $CDCl_3$

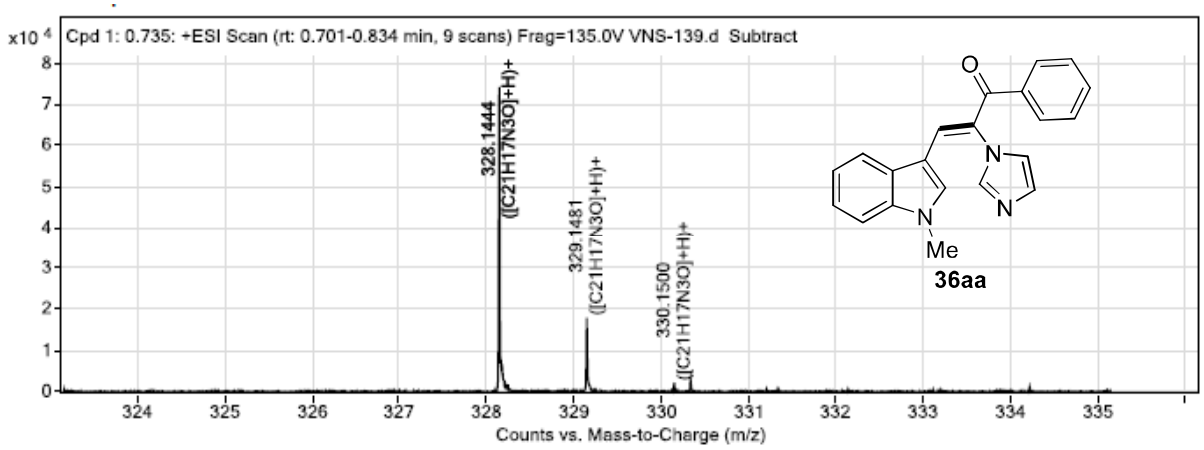

Figure 2.8 LC-HRMS of **36aa**

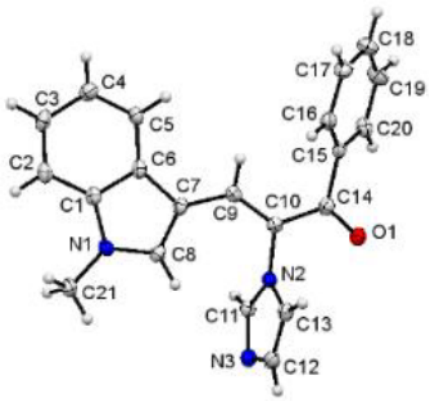

Figure 2.9 Single crystal X-ray of **36aa**

Table 2.2: Optimization of the reaction condition.[a]

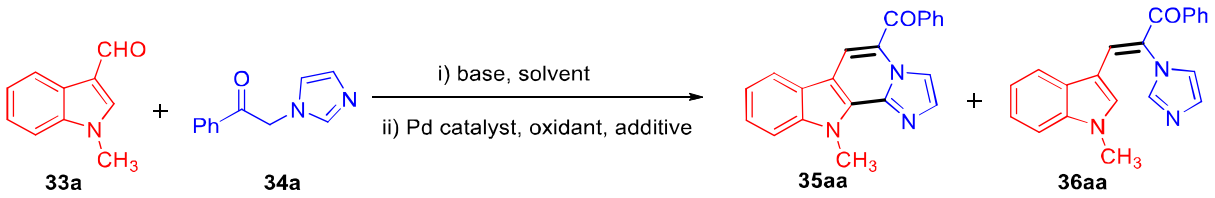

S. No.	Catalyst	Oxidant	Base	Additive	Solvent	Time (h)	% Yield[b]	
							35aa	**36aa**
1	$Pd(OAc)_2$	$Cu(OAc)_2·H_2O$	Piperidine	-	Toluene	30	39	30
2	$Pd(OAc)_2$	$Cu(OAc)_2·H_2O$	Piperidine	AcOH	Toluene	16	82	trace
3	$Pd(OAc)_2$	$Cu(OAc)_2·H_2O$	Pyrrolidine	AcOH	Toluene	30	54	10
4	$Pd(OAc)_2$	$Cu(OAc)_2·H_2O$	Morpholine	AcOH	Toluene	36	77	trace
5	$Pd(OAc)_2$	$Cu(OAc)_2·H_2O$	DBU[c]	AcOH	Toluene	36	traces	10
6	$Pd(OAc)_2$	$Cu(OAc)_2·H_2O$	K_2CO_3	AcOH	Toluene	36	traces	17
7	$PdCl_2$	$Cu(OAc)_2·H_2O$	Piperidine	AcOH	Toluene	16	traces	80
8	$Pd(PPh_3)_4$	$Cu(OAc)_2·H_2O$	Piperidine	AcOH	Toluene	24	20	52
9	$Pd(OAc)_2$	$PhI(OAc)_2$	Piperidine	AcOH	Toluene	24	traces	60
10	$Pd(OAc)_2$	AgOAc	Piperidine	AcOH	Toluene	24	30	20
11	$Pd(OAc)_2$	$K_2S_2O_8$	Piperidine	AcOH	Toluene	24	48	35
12	$Pd(OAc)_2$	$Cu(OAc)_2·H_2O$	Piperidine	PivOH	Toluene	36	30	42
13	$Pd(OAc)_2$	$Cu(OAc)_2·H_2O$	Piperidine	TFA[c]	Toluene	16	65	18
14	$Pd(OAc)_2$	$Cu(OAc)_2·H_2O$	Piperidine	AcOH	Xylene	36	42	32
15	$Pd(OAc)_2$	$Cu(OAc)_2·H_2O$	Piperidine	AcOH	Mesitylene	36	23	40
16	$Pd(OAc)_2$	$Cu(OAc)_2·H_2O$	Piperidine	AcOH	Dioxane	24	0	38
17	$Pd(OAc)_2$	$Cu(OAc)_2·H_2O$	Piperidine	AcOH	DMF	24	0	15
18	$Pd(OAc)_2$	$Cu(OAc)_2·H_2O$	Piperidine	AcOH	DMSO	24	0	10
19	-	$Cu(OAc)_2·H_2O$	Piperidine	AcOH	Toluene	24	0	72
20	$Pd(OAc)_2$	$Cu(OAc)_2·H_2O$	Piperidine	AcOH	Toluene	24	48	28[d]
21	$Pd(OAc)_2$	$Cu(OAc)_2·H_2O$	Piperidine	AcOH	Toluene	24	65	Trace[e]
22	$Pd(OAc)_2$	$Cu(OAc)_2·H_2O$	Piperidine	AcOH	Toluene	24	65	Trace[f]

[a]Reaction conditions: i) **33a** (0.314 mmol), **34a** (0.377 mmol), base (0.477 mmol), solvent (2 mL), 120 °C, 4 h; ii) Pd catalyst (10 mol %), oxidant (50 mol %), additives (20 mol %), solvent (2 mL), 120 °C, 12 h, open air; [b]Isolated yields; [c]DBU = 1,8-Diazabicyclo(5.4.0)undec-7-ene, TFA = Trifluoroacetic acid; [d]Reaction performed under N_2 atm; [e]Reaction performed under O_2 atm. [f]5 mol % $Pd(OAc)_2$ was used.

The above inspiring results indicated the possibility of the envisioned one-pot sequential reaction. Thus, we went on to screen reaction conditions by varying different parameters such as bases, catalysts, oxidants, and additives for the model reactions **(Table 2.2)**. After considerable efforts, the best yield of desired product **35aa** (82%) was observed by performing reaction in the presence of piperidine (2.5 equiv.) in toluene at 120 °C for 4 h followed by the addition of $Pd(OAc)_2$ (10 mol %), $Cu(OAc)_2 \cdot H_2O$ (2 equiv.) and AcOH (20 mol %) and continuing reaction additional 12 h at 120 °C (**Table 2.2,** entry 2).

Also, we performed the reaction under nitrogen atmosphere and observed the **35aa** and **36aa** in 48% and 28% yields, respectively (**Table 2.2,** entry 20). Interestingly, in the oxygen atmosphere, **35aa** was obtained in 63% yield along with trace amount of **36aa**. This experiment revealed that the oxygen plays an important role in this dehydrogenative coupling reaction (**Table 2.2,** entry 21). It is also worth mentioning that the reaction of **33a** and **34a** in piperidine, $Pd(OAc)_2$, $Cu(OAc)_2 \cdot H_2O$ and AcOH in toluene at 120 °C for 24 h in one-pot fashion, gave **32aa** in 55% yield along with **36aa** in 26% yield.

After having optimized reaction condition in hand, we investigated the substrate scope for one-pot sequential protocol **(Table 2.3)**. Initially, *N*-methyl-1*H*-indole-3-carboxaldehyde (**33a**) was treated with substituted active methylene azoles (**34a-l**) to afford corresponding 5-aroyl-11*H*-imidazo[1',2':1,2]pyrido[3,4-*b*]indoles (**35aa-al**) in moderate to excellent (32-86%) yields **(Table 2.3)**. It was observed that active methylene azoles possessing electron-donating groups on aroyl ring furnished better yields as compared to electron-withdrawing groups (compare **35aa-ac** to **35ad-ae**, **Table 2.3**). Remarkably, sterically hindered aryl and heteroaryl moieties were well tolerated to gave corresponding products **35af** and **35ag** in 61% and 80% yields, respectively. The subsequent investigation of substituents on azole ring disclosed that reaction of **33a** with active methylene azoles with methyl group on imidazole ring (**34h-i**) furnished corresponding products **35ah-ai** in excellent yields (83-86%). However, active methylene azoles with diphenyl groups on imidazole (**34j**) and benzimidazole (**34k**) afforded the corresponding products **35aj** (32%) and **35ak** (37%) in moderate yields. Next, substituted *N*-methyl indole-3-carboxaldehydes (**33b-d**) bearing OMe, Br, and CO_2Me groups on the indole ring were reacted with **34a** to successfully furnish corresponding products **35ba** (77%), **35ca** (45%), and **35da** (90%), respectively. In addition, *N*-ethylindole-3-carboxaldehydes (**33e-h**) and *N*-benzylindole-3-carboxaldehydes **(33i-**

l) were treated with **34a** and **34j** to afford corresponding products **35ea-ha** and **35ia-ij** in moderate to good yields. *N*-Benzylindole-3-carboxaldehydes afforded lower yields as compared to *N*-methyl and *N*-ethylindole-3-carboxaldehydes. Interestingly, ester group at C-6 position of *N*-methylindole-3-carboxaldehyde (**33d**) and *N*-ethylindole-3-carboxaldehyde (**33h**) gave the highest yield of the coupled products **35da** and **35ha** in 90% and 94% yields, respectively. Structures of all the synthesized compounds were elucidated with the help of IR, ^{1}H, ^{13}C NMR and HRMS analysis. The structure of compound **35ha** was also cofirmed by single-crystal X-ray crystallography (CCDC No. 1821802) (**Figure 2.10)**. Fascinatingly, *N*-ethylindole-3-carboxaldehyde (**33e**) also reacted with active methylene azole with the isobutyl group (**34m**) under standard reaction condition produce desired product **35em** in moderate yield (38%).

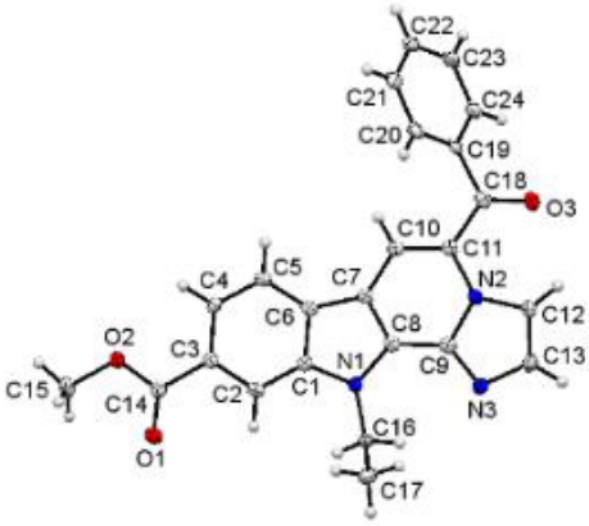

Figure 2.10 Single-crystal X-ray of compound **35ha**

We performed intermolecular competition experiments between of 2-(1*H*-imidazol-1-yl)-1-phenylethan-1-one **(34a)** with 5-methoxy-1-methyl-1*H*-indole-3-carbaldehyde **(33b)** and 5-bromo-1-methyl-1*H*-indole-3-carbaldehyde **(33c)**. The ratio of products **35ba** and **35ca** were 1 : 0.7, which indicated that electron-rich substituents at C5-position of indole reacted preferentially as compared to electron-withdrawing groups.

Table 2.3: Substrate scope for synthesis of 5-aroyl-11*H*-imidazo[1',2':1,2]pyrido[3,4-*b*]indoles (**35**).[a,b]

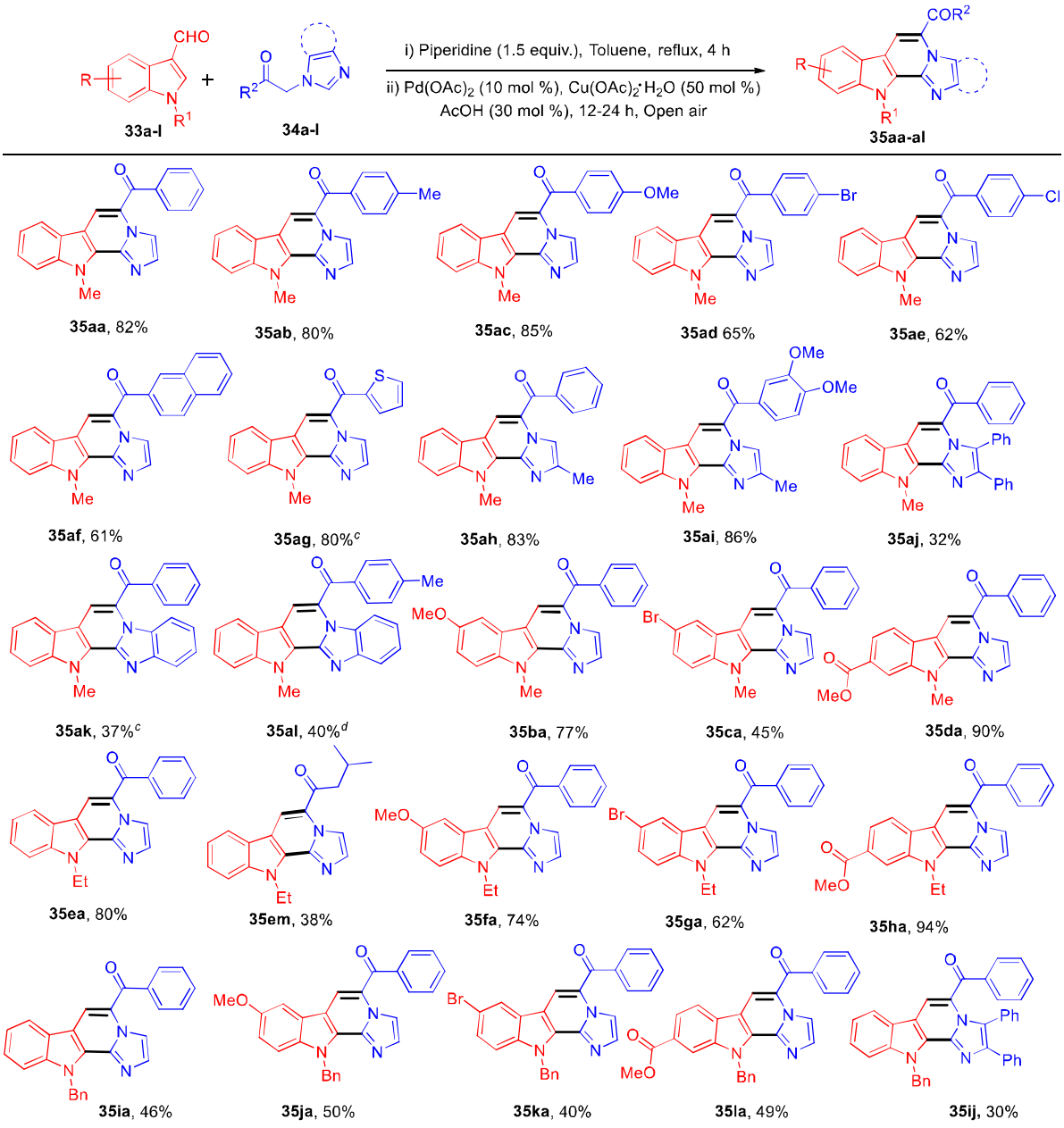

[a]Reaction condition: (i) **33** (0.31 mmol), **34** (0.38 mmol), piperidine (0.47 mmol), Toluene (5 mL), 120 °C, 4 h; (ii) $Pd(OAc)_2$ (21 mg, 10 mol %), $Cu(OAc)_2 \cdot H_2O$ (31 mg, 50 mol %) and AcOH (30 mol %), 12 h. [b]Isolated yields. [c]24 h. [d]20 h.

Next, we probed the substrate scope and check out the generality of the developed protocol for *N*-subtituted-indole-2-carboxaldehydes (**37a-c**) with different active methylene azoles **(Table 2.4)**.

To our delight, 5-aroyl-7*H*-imidazo[1',2':1,2]pyrido[4,3-*b*]indoles (**38aa-ck**) were obtained in moderate to excellent (23-82%) yields. As earlier mentioned, coupled products *N*-benzylindole-2-carboxaldehydes resulted in lower yields than *N*-methylindole-2-carboxaldehydes. When *N*-ethylindole-3-carbaldehyde (**33e**) and *N*-ethylindole-2-carabaldehyde (**37b**) reacted with **34a** revealed that **33e** reacted faster as compared to **37b** furnishing **35ea** and **38ba** in 40% and 25% yields, respectively.

Table 2.4: Substrate scope for synthesis of 5-aroyl-7*H*-imidazo[1',2':1,2]pyrido[4,3-*b*]indoles (**38**).[a]

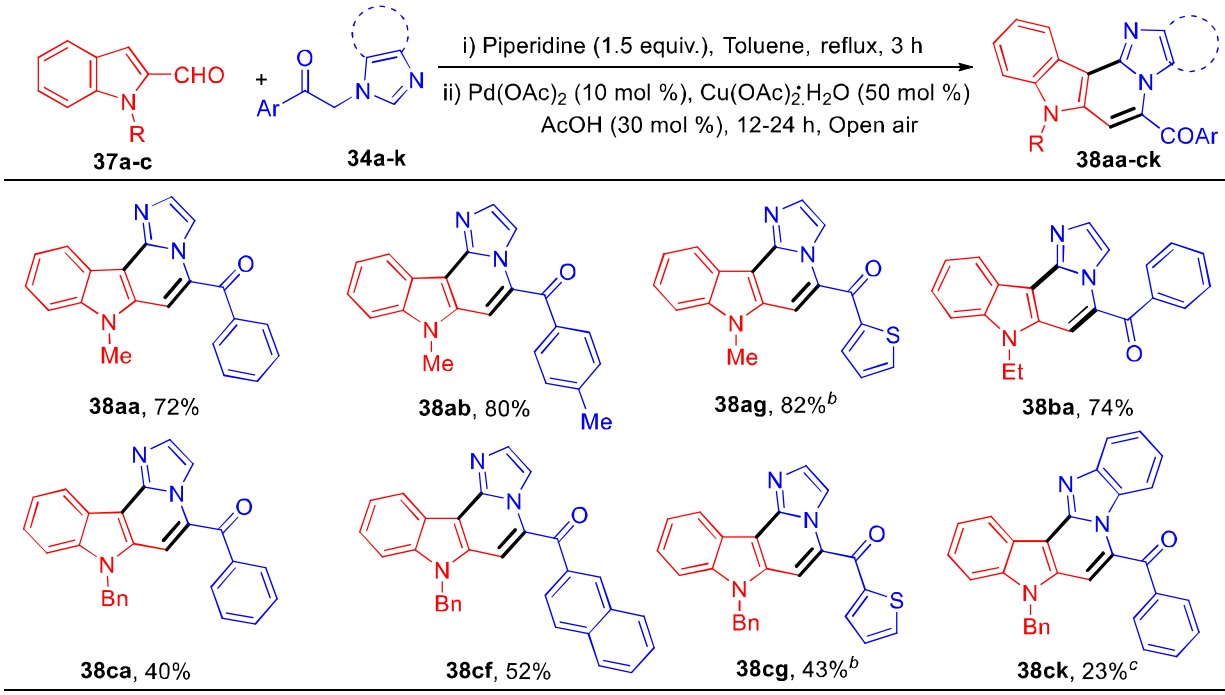

[a]Reaction condition: (i) **37** (0.32 mmol), **34** (0.38 mmol), piperidine (0.47 mmol), toluene (5 mL), 120 °C, 3 h; (ii) $Pd(OAc)_2$ (10 mol %), $Cu(OAc)_2 \cdot H_2O$ (50 mol %) and AcOH (30 mol %), 12 h, open air. [b]24 h. [c]20 h.

The developed synthetic strategy was further extended for the reaction of thiophene-2-carboxaldehyde (**39a**) with active methylene azoles (**34a** and **34c**). To our delight, desired 5-aroyl-imidazo[1,2-*a*]thieno[3,2-*c*]pyridines **40aa** (38%) and **40ac** (43%) were isolated in moderate yields under standard reaction condition **(Scheme 2.14)**. Likewise, benzofuran-3-carbaldehyde (**41**) also reacted under the optimized reaction condition with active methylene azoles (**34a)** to afford the benzofuro[2,3-*c*]imidazo[1,2-*a*]pyridin-5-yl(phenyl)methanone (**42**) in 34% yield.

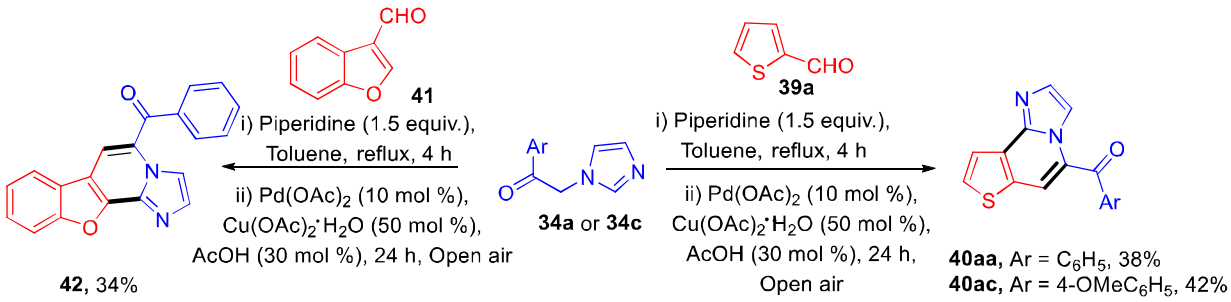

Scheme 2.14. Synthesis of 5-aroyl-imidazo[1,2-*a*]thieno[3,2-*c*]pyridines **(40)** and 5- aroyl-benzofuro[2,3-*c*]imidazo[1,2-*a*]pyridine **(42)**

To determined the practicality and efficiency of the derived protocol, a scaled-up experiment was carried out. The desired product **35aa** was obtained in 78% (1.59 g) yield from a gram-scale reaction of **33a** with **34a** under the optimized reaction conditions **(Scheme 2.15)**.

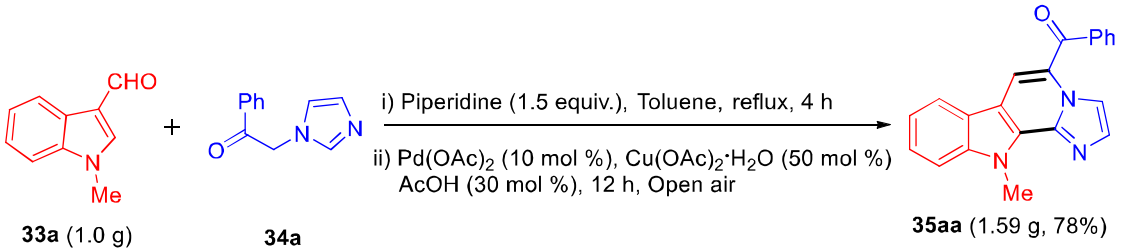

Scheme 2.15. Gram scale reaction for synthesis of **35aa**

To gain insight into the mechanism of one-pot sequential reaction, some control experiments were performed **(Scheme 2.16)**. The compound **33a** was reacted with **34a** under standard reaction condition in the presence of TEMPO and BHT radical inhibitors **(Scheme 2.16A)**. Under this condition **35aa** was obtained 77% and 79% yields, respectively, thus the possibility of the radical pathway was ruled out. Next, **33a** was reacted with **34a** using piperidine in toluene and Knoevenagel condensation product **36aa** was isolated in 92% yield which was then subjected to dehydrogenative coupling using $Pd(OAc)_2$ and $Cu(OAc)_2{\cdot}H_2O$ to give the coupled product **35aa** in 82% yield **(Scheme 2.16B)**. Lastly, to comprehend the reactivity of C2 indole and C2 imidazole protons, the reaction of intermediate **36aa** was treated with 4-iodoanisole **(43)** in presence of $Pd(OAc)_2$ and AgOAc **(Scheme 2.16C)**. From this reaction intermolecular direct arylation product at C2-position of imidazole, 3-(1*H*-indol-3-yl)-2-(2-(4-methoxyphenyl)-1*H*-imidazol-1-yl)-1-

phenylprop-2-en-1-one **(44)** was obtained in 10% yield along with **35aa**. This experiment defined that palladation preferentially occur at C2-position of imidazole.

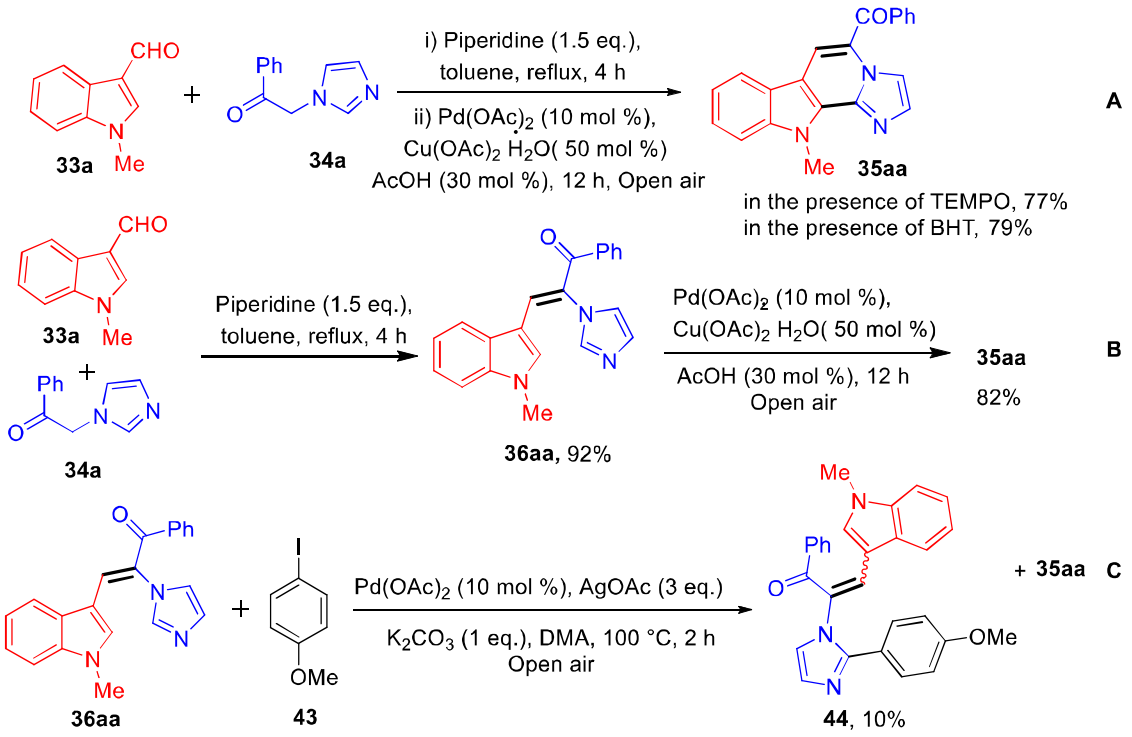

Scheme 2.16. Control experiments

Based on the experimental results and literature reports[24, 27] a tentative mechanism for this one-pot sequential reaction is proposed (**Scheme 2.17)**. Firstly, Knoevenagel adduct **36aa** is formed by the reaction of **33a** with **34a** in the presence of piperidine. Then Knoevenagel adduct **36aa** undergoes regioselective palladation at C2 position of imidazole to formed intermediate **I.** Subsequently, intermediate **II** is formed *via* C–H bond cleavage through concerted metalation-deprotonation process. Lastly, intermediate **II** undergoes reductive elimination resulted the coupled product **35aa**.

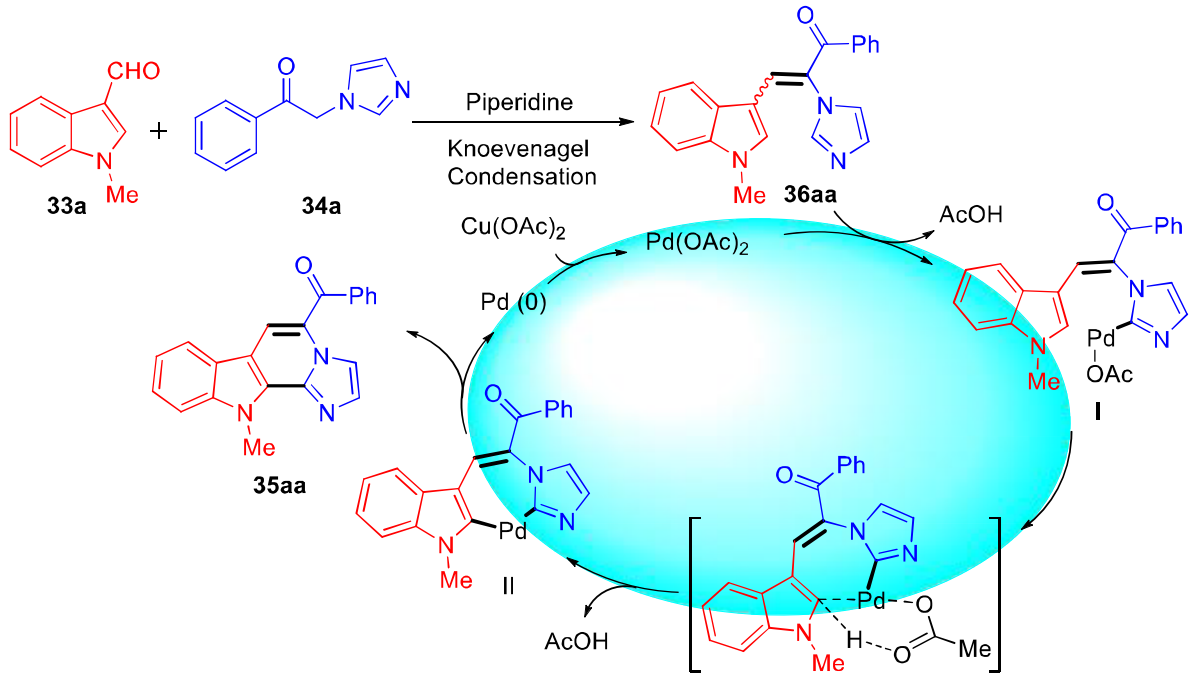

Scheme 2.17. Proposed mechanism

2.3 CONCLUSION

In summary, we have developed a new efficient approach towards the synthesis of novel imidazopyridine-fused indoles. The designed strategy involves one-pot sequential Knoevenagel condensation of readily accessible active methylene azoles with *N*-substituted-1*H*-indole-3-carboxaldehydes or *N*-substituted- 1*H*-indole-2-carboxaldehydes followed by palladium-catalyzed intramolecular cross-dehydrogenative coupling reaction. The method showed broad substrate scope with tolerance of various functional groups and amiable for gram-scale preparation without problems. The developed protocol opens up ways for the synthesis of aroyl substituted polycyclic *N*-heterocyles which could provide a new class of medicinally relevant indole-based heterocycles.

2.4 EXPERIMENTAL SECTION

2.4.1 General Materials and Methods

All the reagents and solvents were obtained from the commercial suppliers and used without further purification unless otherwise stated. The active methylene azoles (**34a-m)** were synthesized by literature reports.[34] Progress of the reaction was monitored by Thin Layer Chromatography

(TLC) on 0.2 mm silica gel F_{254} plates. All synthesized products were purified by column chromatography on silica gel (100-200 mesh). All ^{1}H and ^{13}C NMR spectra were recorded on 400 MHz and 100 MHz spectrometer respectively in $CDCl_3$ solvent. Chemical shift (δ) reported in ppm and coupling constant (J) reported in Hz using tetramethylsilane (TMS) as an internal reference. IR spectra were recorded as a neat sample on a FT-IR instrument and values are expressed in cm^{-1}. The HRMS data were recorded on Q-TOF LC-MS spectrometer by electrospray ionization (ESI) method. Melting points were determined in open capillary tubes on an automated melting apparatus and are uncorrected.

2.4.2 General Procedure for the Synthesis of Imidazopyridine Fused Indoles. A 10 mL RB flask was chared with 1-methyl-1*H*-indole-3-carbaldehyde **(33a)** (50 mg, 0.314 mmol), 2-(1*H*-imidazol-1-yl)-1-phenylethan-1-one **(34a)** (70 mg, 0.377 mmol), piperidine (40 mg, 0.471 mmol) in toluene (1 mL) at 120 °C for 4 h in oil bath. Thereafter, $Pd(OAc)_2$ (21 mg, 0.031 mmol), $Cu(OAc)_2.H_2O$ (31 mg, 0.157 mmol) and AcOH (0.3 ml) were added to the reaction mixture and heated at 120 °C for 12 h. After consumption of starting materials, toluene evaporated on reduced pressure and residue purified by colomn chromatography (10% *v/v* EtOAc: hexane) to afford desired product **35aa** in 82% (84 mg) yield.

(11-Methyl-11*H*-imidazo[1',2':1,2]pyrido[3,4-*b*]indol-5-yl)(phenyl)methanone (35aa):

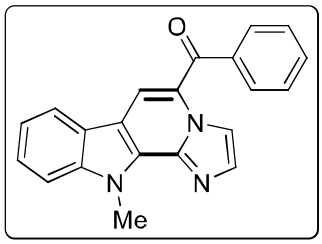

Yellow solid (84 mg, 82%); m.p. 195-197 °C; ^{1}H NMR (400 MHz, Chloroform-*d*) δ 9.20 (d, *J* = 1.3 Hz, 1H), 8.09 (s, 1H), 7.94 (d, *J* = 7.9 Hz, 1H), 7.89 – 7.86 (m, 2H), 7.84 (d, *J* = 1.4 Hz, 1H), 7.71 – 7.67 (m, 1H), 7.62 – 7.57 (m, 3H), 7.54 (td, *J* = 6.8, 1.2 Hz, 1H), 7.37 – 7.33 (m, 1H), 4.59 (s, 3H); $^{13}C\{^{1}H\}$ NMR (100 MHz, Chloroform-*d*) δ 189.8, 140.7, 139.0, 137.2, 132.5, 132.0, 131.3, 129.7, 128.5, 125.7, 125.5, 123.2, 121.5, 119.8, 119.6, 116.3, 113.0, 110.2, 32.2; FT-IR ν_{max} (neat) 2350, 1615, 1520, 1260, 740 cm^{-1}; HRMS (ESI) calcd for $C_{21}H_{16}N_3O$ $[M + H]^+$: 326.1288, found 326.1305.

(11-Methyl-11*H*-imidazo[1',2':1,2]pyrido[3,4-*b*]indol-5-yl)(*p*-tolyl)methanone (35ab):

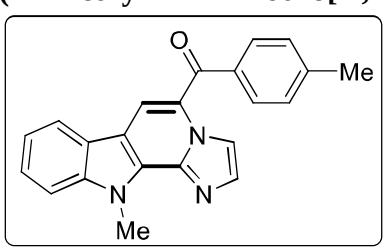

Yellow solid (85 mg, 80%); m.p. 208-210 °C; ^{1}H NMR (400 MHz, Chloroform-*d*) δ 9.12 (bs, 1H), 8.06 (s, 1H), 7.93 (d, *J* = 7.9 Hz, 1H), 7.81 – 7.77 (m, 3H), 7.56 – 7.50 (m, 2H), 7.39 (d, *J* = 8.0 Hz, 2H), 7.34 (t, *J* = 7.6 Hz, 1H), 4.56 (s, 3H), 2.53 (s, 3H);

$^{13}C\{^{1}H\}$ NMR (100 MHz, Chloroform-*d*) δ 189.6, 142.8, 140.7, 137.2, 136.1, 132.3, 131.0, 129.9, 129.2, 125.6, 123.2, 121.4, 119.8, 119.1, 116.2, 113.0, 110.2, 32.1, 21.7; FT-IR ν_{max} (neat) 2360, 1620, 1545, 1240, 720 cm^{-1}; HRMS (ESI) calcd for $C_{22}H_{18}N_3O$ $[M + H]^+$: 340.1444, found 340.1440.

(4-Methoxyphenyl)(11-methyl-11*H*-imidazo[1',2':1,2]pyrido[3,4-*b*]indol-5-yl)methanone

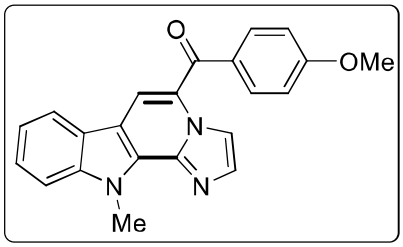

(35ac): Yellow solid (94 mg, 85%); m.p. 230-232 °C; ^{1}H NMR (400 MHz, Chloroform-*d*) δ 9.03 (s, 1H), 8.06 (s, 1H), 7.97 (d, *J* = 7.9 Hz, 1H), 7.91 (d, *J* = 8.4 Hz, 2H), 7.82 (s, 1H), 7.60 – 7.52 (m, 2H), 7.36 (t, *J* = 7.4 Hz, 1H), 7.09 (d, *J* = 8.4 Hz, 2H), 4.59 (s, 3H), 3.97 (s, 3H); $^{13}C\{^{1}H\}$ NMR (100 MHz, Chloroform-*d*) δ 188.8, 163.1, 140.7, 137.3, 132.3, 132.1, 131.2, 130.9, 125.8, 125.6, 123.2, 121.3, 119.8, 118.3, 116.1, 113.9, 113.0, 110.2, 55.6, 32.2; FT-IR ν_{max} (neat) 2315, 1663, 1558, 1287, 741 cm^{-1}; HRMS (ESI) calcd for $C_{22}H_{18}N_3O_2$ $[M + H]^+$: 356.1394; found 356.1386.

(4-Bromophenyl)(11-methyl-11*H*-imidazo[1',2':1,2]pyrido[3,4-*b*]indol-5-yl)methanone

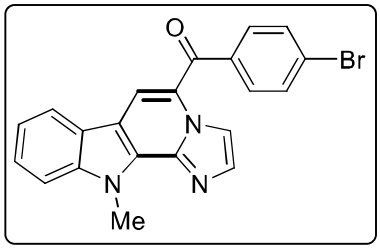

(35ad): Yellow solid (83 mg, 65%); m.p. 228-230 °C; ^{1}H NMR (400 MHz, Chloroform-*d*) δ 9.17 (d, *J* = 1.2 Hz, 1H), 8.05 (bs, 1H), 7.97 (d, *J* = 7.8 Hz, 1H), 7.85 (d, *J* = 1.6 Hz, 1H), 7.75 (s, 4H), 7.61 – 7.53 (m, 2H), 7.38 (t, *J* = 6.4 Hz, 1H), 4.60 (s, 3H); $^{13}C\{^{1}H\}$ NMR (100 MHz, Chloroform-*d*) δ 188.5, 140.7, 137.8, 137.1, 132.7, 131.8, 131.2, 129.7, 128.5, 126.9, 125.8, 125.1, 123.1, 121.6, 119.8, 119.6, 116.3, 113.0, 110.2, 32.2; FT-IR ν_{max} (neat) 2345, 1615, 1520, 1215, 780 cm^{-1}; HRMS (ESI): calcd for $C_{21}H_{15}BrN_3O$ $[M + H]^+$: 404.0393; found, 404.0385 and 406.0375.

(4-Chlorophenyl)(11-methyl-11*H*-imidazo[1',2':1,2]pyrido[3,4-*b*]indol-5-yl)methanone

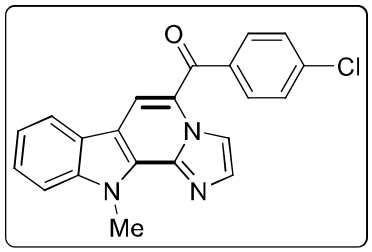

(35ae): Yellow solid (70 mg, 62%); m.p. 218-220 °C; ^{1}H NMR (400 MHz, Chloroform-*d*) δ 9.17 (d, *J* = 1.3 Hz, 1H), 8.06 (s, 1H), 7.97 (d, *J* = 7.8 Hz, 1H), 7.85 (s, 1H), 7.83 (d, *J* = 8.4 Hz, 2H), 7.59 – 7.56 (m, 4H), 7.38 (t, *J* = 7.3 Hz, 1H), 4.60 (s, 3H); $^{13}C\{^{1}H\}$ NMR (100 MHz, Chloroform-*d*) δ 188.4, 140.8, 138.4, 137.3, 132.7, 131.4, 131.0, 128.9, 125.9, 125.2, 123.2, 121.6, 119.9, 119.6, 116.3, 113.1, 110.3, 32.2; FT-

IR ν_{max} (neat) 2260, 1630, 1580, 1260, 680 cm^{-1}; HRMS (ESI) calcd for $C_{21}H_{15}ClN_3O$ $[M + H]^+$: 360.0898, found 360.0891.

(11-Methyl-11*H*-imidazo[1',2':1,2]pyrido[3,4-*b*]indol-5-yl)(naphthalen-2-yl)methanon

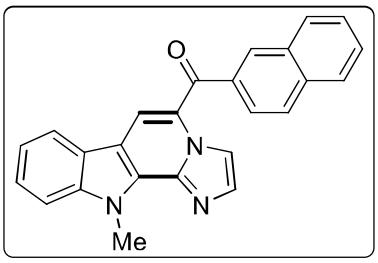

(35af): Yellow solid (72 mg, 61%); m.p. 202-204 °C; ^{1} NMR (400 MHz, Chloroform-*d*) δ 9.21 (d, *J* = 1.3 Hz, 1H), 8.36 (s, 1H), 8.17 (s, 1H), 8.07 (d, *J* = 8.5 Hz, 1H), 8.02 – 7.97 (m, 3H), 7.91 (d, *J* = 7.8 Hz, 1H), 7.87 (d, *J* = 1.3 Hz, 1H), 7.71 – 7.68 (m, 1H), 7.66 – 7.59 (m, 2H), 7.54 (t, *J* = 8.0 Hz, 1H), 7.34 (t, *J* = 7.5 Hz, 1H), 4.62 (s, 3H); $^{13}C\{^1H\}$ NMR (100 MHz, Chloroform-*d*) δ 189.8, 140.8, 137.2, 136.2, 135.0, 132.6, 132.4, 131.3, 130.8, 129.3, 128.6, 128.3, 127.9, 127.1, 125.8, 125.7, 123.2, 121.5, 119.9, 119.6, 116.3, 113.1, 110.2, 32.2; FT-IR ν_{max} (neat) 2390, 1670, 1530, 1280 cm^{-1}; HRMS (ESI) calcd for $C_{25}H_{18}N_3O$ $[M + H]^+$: 376.1444, found 376.1439.

(11-Methyl-11*H*-imidazo[1',2':1,2]pyrido[3,4-*b*]indol-5-yl)(thiophen-2-yl)methanone (35ag):

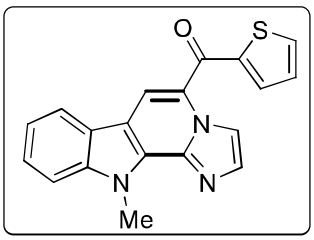

Yellow solid (83 mg, 80%); m.p. 168-170 °C; ^{1}H NMR (400 MHz, Chloroform-*d*) δ 8.94 (d, *J* = 1.4 Hz, 1H), 8.39 (s, 1H), 8.04 (d, *J* = 7.9 Hz, 1H), 7.83 (s, 1H), 7.82 – 7.80 (m, 2H), 7.62 – 7.55 (m, 3H), 7.42 – 7.38 (m, 1H), 4.60 (s, 3H); ^{13}C NMR (100 MHz, Chloroform-*d*) δ 181.2, 143.7, 140.7, 137.2, 133.8, 133.7, 132.4, 128.0, 125.7, 123.3, 121.5, 119.9, 117.4, 115.9, 113.1, 110.2, 32.2; FT-IR ν_{max} (neat) 2340, 1635, 1510, 1270 cm^{-1}; HRMS (ESI) calcd for $C_{19}H_{14}N_3OS$ $[M + H]^+$: 332.0852, found 332.0847.

(2,11-Dimethyl-11*H*-imidazo[1',2':1,2]pyrido[3,4-*b*]indol-5-yl)(phenyl)methanone (35ah):

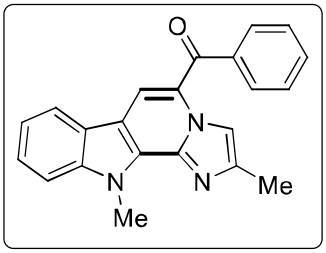

Yellow solid (88 mg, 83%); m.p. 198-200 °C; ^{1}H NMR (400 MHz, Chloroform-*d*) δ 8.93 (d, *J* = 1.0 Hz, 1H), 8.02 (s, 1H), 7.92 (d, *J* = 7.9 Hz, 1H), 7.87 – 7.85 (m, 2H), 7.68 (tt, *J* = 7.2, 1.2 Hz, 1H), 7.61 – 7.57 (m, 2H), 7.55 – 7.50 (m, 2H), 7.36 – 7.32 (m, 1H), 4.58 (s, 3H), 2.63 (s, 3H); $^{13}C\{^1H\}$ NMR (100 MHz, Chloroform-*d*) δ 189.8, 142.5, 140.8, 139.2, 136.6, 131.9, 130.8, 129.7, 128.5, 125.6, 125.1, 123.3, 121.3, 119.8, 119.0, 113.5, 113.0, 110.1, 32.2, 14.7; FT-IR ν_{max} (neat) 2360, 1690, 1480, 1245 cm^{-1}; HRMS (ESI) calcd for $C_{22}H_{18}N_3O$ $[M+H]^+$: 340.1444, found 340.1445.

(3,4-Dimethoxyphenyl)(3,11-dimethyl-11*H*-imidazo[1',2':1,2]pyrido[3,4-*b*]indol-5-yl)ethanone (35ai): 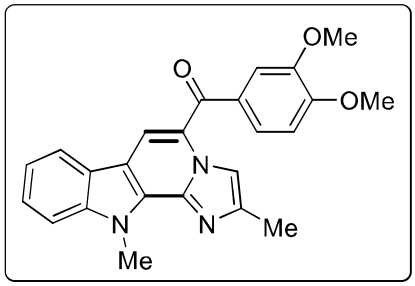

Yellow solid (107 mg, 86%); m.p. 198-199 °C; ^{1}H NMR (400 MHz, Chloroform-*d*) δ 8.73 (s, 1H), 8.02 (s, 1H), 7.95 (d, *J* = 7.8 Hz, 1H), 7.57 – 7.47 (m, 4H), 7.36 – 7.32 (m, 1H), 7.01 (d, *J* = 8.3 Hz, 1H), 4.58 (s, 3H), 4.04 (s, 3H), 4.00 (s, 3H), 2.61 (s, 3H); ^{13}C{^{1}H} NMR (100 MHz, Chloroform-*d*) δ 188.8, 152.8, 149.2, 142.1, 140.7, 136.7, 131.4, 130.5, 125.5, 125.4, 124.5, 123.3, 121.2, 119.7, 117.5, 113.2, 113.0, 112.3, 110.1, 110.0, 56.2, 56.1, 32.2, 14.7; FT-IR ν_{max} (neat) 2360, 1627, 1504, 1257, 763 cm^{-1}; HRMS (ESI) calcd for $C_{24}H_{22}N_3O_3$ $[M + H]^+$: 400.1656, found 400.1674.

(11-Methyl-2,3-diphenyl-11*H*-imidazo[1',2':1,2]pyrido[3,4-*b*]indol-5-yl)(phenyl)methanone (35aj): 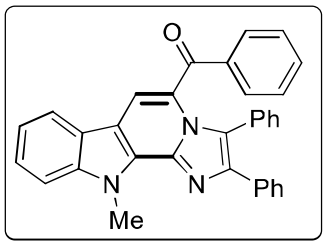

Yellow solid (48 mg, 32%); m.p. 175-176 °C; ^{1}H NMR (400 MHz, Chloroform-*d*) δ 7.99 (d, *J* = 7.9 Hz, 1H), 7.75 (s, 1H), 7.63 (t, *J* = 9.3 Hz, 3H), 7.57 – 7.47 (m, 3H), 7.41 – 7.35 (m, 5H), 7.28 – 7.24 (m, 2H), 7.23 – 7.15 (m, 3H), 7.11 (d, *J* = 7.3 Hz, 2H), 4.70 (s, 3H); ^{13}C{^{1}H} NMR (100 MHz, Chloroform-*d*) δ 188.3, 141.7, 140.7, 137.2, 136.7, 134.5, 132.8, 131.5, 129.9, 129.6, 129.2, 129.0, 128.4, 128.3, 128.2, 128.1, 127.3, 125.4, 124.3, 123.2, 121.0, 119.9, 113.8, 113.4, 110.0, 32.2; FT-IR ν_{max} (neat) 2350, 1610, 1504, 1257, 740 cm^{-1}; HRMS (ESI) calcd for $C_{33}H_{24}N_3O$ $[M + H]^+$: 478.1914, found 478.1915.

(12-Methyl-12*H*-benzo[4',5']imidazo[1',2':1,2]pyrido[3,4-*b*]indol-6-yl)(phenyl)methanone (35ak): 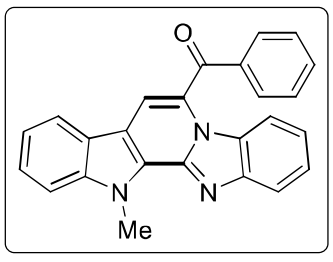

Yellow solid (44 mg, 37%); m.p. 274-276 °C; ^{1}H NMR (400 MHz, Chloroform-*d*) δ 8.16 (d, *J* = 7.2 Hz, 2H), 8.06 (d, *J* = 8.2 Hz, 1H), 7.98 (d, *J* = 7.9 Hz, 1H), 7.81 (s, 1H), 7.78 – 7.75 (m, 2H), 7.65 – 7.61 (m, 3H), 7.58 (t, *J* = 7.6 Hz, 1H), 7.53 (t, *J* = 7.8 Hz, 1H), 7.39 (t, *J* = 7.6 Hz, 1H), 7.32 (t, *J* = 7.6 Hz, 1H), 4.73 (s, 3H); ^{13}C{^{1}H} NMR (100 MHz, Chloroform-*d*) δ 188.3, 144.4, 141.5, 141.0, 137.1, 133.8, 130.7, 129.6, 129.4, 128.7, 126.1, 124.9, 122.9, 121.7, 121.4, 120.2, 120.0, 115.3, 115.1, 114.6, 110.4, 32.4; FT-IR ν_{max} (neat) 2350, 1635, 1510, 1257, 740 cm^{-1}; HRMS (ESI) calcd for $C_{25}H_{18}N_3O$ $[M+H]^+$: 376.1444, found 376.1459.

(12-Methyl-12*H*-benzo[4',5']imidazo[1',2':1,2]pyrido[3,4-*b*]indol-6-yl)(*p*-tolyl)methanone

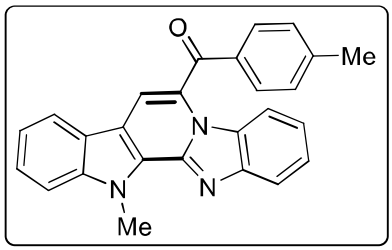

(35al): Yellow solid (49 mg, 40%); m.p. 224-225 °C; ^{1}H NMR (400 MHz, Chloroform-*d*) δ 8.07 – 8.04 (m, 3H), 7.99 (d, *J* = 7.9 Hz, 1H), 7.78 (s, 1H), 7.74 (d, *J* = 8.4 Hz, 1H), 7.64 (d, *J* = 8.4 Hz, 1H), 7.60 – 7.55 (m, 1H), 7.54 – 7.50 (m, 1H), 7.42 (d, *J* = 7.9 Hz, 2H), 7.39 – 7.35 (m, 1H), 7.33 – 7.30 (m, 1 H), 4.73 (s, 3H), 2.54 (s, 3H); ^{13}C{^{1}H} NMR (100 MHz, Chloroform-*d*) δ 188.2, 145.0, 140.9, 134.4, 130.9, 130.8, 129.6, 129.5, 126.1, 124.8, 122.9, 122.7, 121.6, 121.3, 120.1, 119.9, 115.2, 115.1, 113.8, 113.7, 110.4, 32.4, 21.9; FT-IR ν_{max} (neat) 2360, 1640, 1540, 1280, 770 cm^{-1}; HRMS (ESI) calcd for $C_{26}H_{20}N_3O$ [M + H]$^{+}$: 390.1601, found 390.1613.

(8-Methoxy-11-methyl-11*H*-imidazo[1',2':1,2]pyrido[3,4-*b*]indol-5-yl)(phenyl)methanone

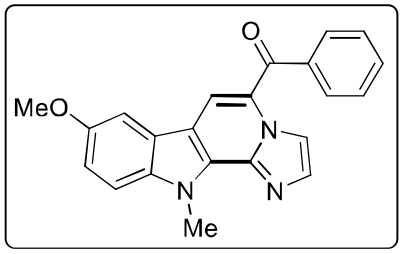

(35ba): Yellow solid (73 mg, 77%); m.p. 205-206 °C; ^{1}H NMR (400 MHz, Chloroform-*d*) δ 9.18 (d, *J* = 1.3 Hz, 1H), 8.06 (s, 1H), 7.90 – 7.87 (m, 2H), 7.83 (d, *J* = 1.3 Hz, 1H), 7.72 – 7.68 (m, 1H), 7.63 – 7.59 (m, 2H), 7.48 (d, *J* = 8.9 Hz, 1H), 7.37 (d, *J* = 2.4 Hz, 1H), 7.17 (dd, *J* = 8.9, 2.4 Hz, 1H), 4.57 (s, 3H), 3.92 (s, 3H); ^{13}C{^{1}H} NMR (100 MHz, Chloroform-*d*) δ 189.7, 155.5, 139.1, 137.2, 135.7, 132.4, 131.9, 131.6, 129.7, 128.5, 125.1, 123.8, 119.8, 116.3, 115.3, 112.8, 111.0, 102.2, 56.1, 32.3.; FT-IR ν_{max} (neat) 2370, 1685, 1290, 790 cm^{-1}; HRMS (ESI) calcd for $C_{22}H_{18}N_3O_2$ [M + H]$^{+}$: 356.1394, found 356.1403.

(8-Bromo-11-methyl-11*H*-imidazo[1',2':1,2]pyrido[3,4-*b*]indol-5-yl)(phenyl)methanone

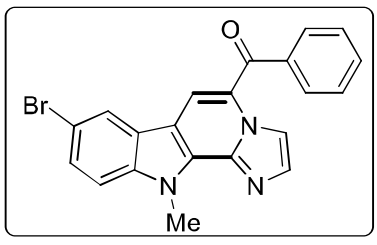

(35ca)*:* Yellow solid (38 mg, 45%); m.p. 252-254 °C; ^{1}H NMR (400 MHz, Chloroform-*d*) ^{1}H NMR (400 MHz, Chloroform-*d*) δ 9.17 (d, *J* = 1.4 Hz, 1H), 8.05 (d, *J* = 1.9 Hz, 1H), 8.00 (s, 1H), 7.87 – 7.84 (m, 3H), 7.70 (t, *J* = 7.4 Hz,, 1H), 7.63 – 7.59 (m, 3H), 7.44 (d, *J* = 8.7 Hz, 1H), 4.56 (s, 3H); ^{13}C{^{1}H} NMR (100 MHz, Chloroform-*d*) δ 189.8, 139.4, 138.7, 136.9, 132.8, 132.2, 131.6, 129.6, 128.6, 128.4, 125.8, 124.8, 122.6, 119.2, 116.5, 114.6, 112.0, 111.6, 32.3; FT-IR ν_{max} (neat) 2325, 1620, 1270, 710 cm^{-1}; HRMS (ESI) calcd for $C_{21}H_{15}BrN_3O$ [M + H]$^{+}$: 404.0393, found 404.0392 and 406.0373.

Methyl-5-benzoyl-11-methyl-11*H*-imidazo[1',2':1,2]pyrido[3,4-*b*]indole-9-carboxylate

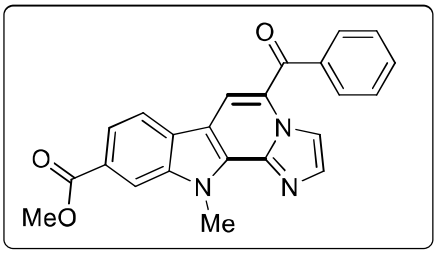

(35da): Yellow solid (79 mg, 90%); m.p. 215-217 °C; ^{1}H NMR (400 MHz, Chloroform-*d*) δ 9.17 (d, *J* = 1.3 Hz, 1H), 8.32 (dd, *J* = 1.4, 0.7 Hz, 1H), 8.08 (s, 1H), 8.04 (dd, *J* = 8.3, 1.4 Hz, 1H), 7.97 (dd, *J* = 8.3, 0.7 Hz, 1H), 7.89 – 7.88 (m, 1H), 7.87 – 7.86 (m, 2H), 7.70 (tt, *J* = 7.6, 1.2 Hz, 1H), 7.61 (tt, *J* = 7.6, 1.2 Hz, 2H), 4.65 (s, 3H), 4.02 (s, 3H); ^{13}C{^{1}H} NMR (100 MHz, Chloroform-*d*) δ 189.8, 167.3, 140.2, 138.7, 136.9, 132.9, 132.3, 129.7, 128.6, 127.1, 126.8, 126.0, 122.5, 119.5, 119.4, 116.8, 112.4, 112.2, 52.4, 32.4; FT-IR ν_{max} (neat) 2370, 1690, 1230, 740 cm^{-1}; HRMS (ESI) calcd for $C_{23}H_{18}N_3O_3$ [M + H]$^{+}$: 384.1343, found 384.1349.

(11-Ethyl-11*H*-imidazo[1',2':1,2]pyrido[3,4-*b*]indol-5-yl)(phenyl)methanone (35ea): Yellow solid (79 mg, 80%); m.p. 274-276 °C; ^{1}H NMR (400 MHz, Chloroform-*d*) δ 9.20 (d, *J* = 1.4 Hz, 1H), 8.10 (s, 1H), 7.96 (d, *J* = 7.9 Hz, 1H), 7.91 – 7.83 (m, 3H), 7.71 – 7.67 (m, 1H), 7.63 – 7.58 (m, 3H), 7.55 – 7.51 (m, 1H), 7.35 (t, *J* = 7.5 Hz, 1H), 5.17 (q, *J* = 7.2 Hz, 2H), 1.63 (t, *J* = 7.1 Hz, 3H); ^{13}C{^{1}H} NMR (100 MHz, Chloroform-*d*) δ 189.8, 139.6, 139.0, 136.8, 132.7, 132.0, 130.5, 129.7, 128.5, 125.6, 125.5, 123.5, 121.3, 120.0, 119.6, 116.3, 113.2, 110.3, 40.4, 15.2; FT-IR ν_{max} (neat) 2350, 1645, 1225, 770 cm^{-1}; HRMS (ESI) calcd for $C_{22}H_{18}N_3O$ [M + H]$^{+}$: 340.1444, found 340.1445.

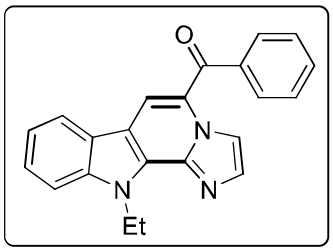

1-(11-Ethyl-11*H*-imidazo[1',2':1,2]pyrido[3,4-*b*]indol-5-yl)-3-methylbutan-1-one (35em): Red solid (35 mg, 38%); m.p. 103-104 °C; ^{1}H NMR (400 MHz, Chloroform-*d*) δ 9.39 (s, 1H), 8.36 (s, 1H), 8.09 (d, *J* = 7.8 Hz, 1H), 7.80 (d, *J* = 1.4 Hz, 1H), 7.55 (dt, *J* = 15.0, 8.0 Hz, 2H), 7.47 – 7.34 (m, 1H), 5.08 (q, *J* = 7.2 Hz, 2H), 3.04 (d, *J* = 7.0 Hz, 2H), 2.45 (dp, *J* = 13.5, 6.7 Hz, 1H), 1.58 (t, *J* = 7.1 Hz, 3H), 1.12 (d, *J* = 6.7 Hz, 6H); ^{13}C{^{1}H} NMR (100 MHz, Chloroform-*d*) δ 193.1, 139.6, 136.7, 132.6, 130.5, 125.9, 125.5, 123.4, 121.2, 119.7, 116.6, 115.5, 112.9, 110.2, 47.3, 40.2, 26.1, 22.9, 15.1; FT-IR ν_{max} (neat) 1658, 1504, 1411, 1288, 1203, 732 cm^{-1}; HRMS (ESI) calcd for $C_{20}H_{22}N_3O$ [M + H]$^{+}$: 320.1757, found 320.1754.

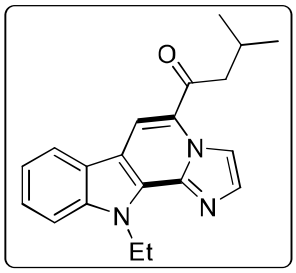

(11-Ethyl-8-methoxy-11*H*-imidazo[1',2':1,2]pyrido[3,4-*b*]indol-5-yl)(phenyl)methanone

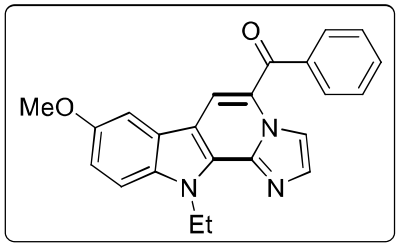

(35fa): Yellow solid (67 mg, 74 %); m.p. 210-212 °C; ^{1}H NMR (400 MHz, Chloroform-*d*) δ 9.19 (s, 1H), 8.16 (s, 1H), 7.94 (s, 1H), 7.90 (d, *J* = 7.6 Hz, 2H), 7.73 (t, *J* = 7.3 Hz, 1H), 7.63 (t, *J* = 7.2 Hz, 2H), 7.56 (d, *J* = 8.7 Hz, 1H), 7.41 – 7.40 (m,1H), 7.23 (d, *J* = 8.1 Hz, 1H), 5.20 – 5.19 (m, 2H), 3.93 (s, 3H), 1.64 (bs, 3H); ^{13}C{^{1}H} NMR (100 MHz, Chloroform-*d*) δ 189.4, 155.8, 138.5, 135.1, 135.0, 134.9, 132.5, 129.9, 128.7, 124.9, 123.6, 120.0, 116.7, 116.7, 116.4, 111.6, 102.2, 56.1, 41.0, 15.8; FT-IR ν_{max} (neat) 2355, 1670, 1225, 790 cm^{-1}; HRMS (ESI) calcd for $C_{23}H_{20}N_3O_2$ [M + H]$^{+}$: 370.1550, found 370.1552.

(8-Bromo-11-ethyl-11*H*-imidazo[1',2':1,2]pyrido[3,4-*b*]indol-5-yl)(phenyl)methanone

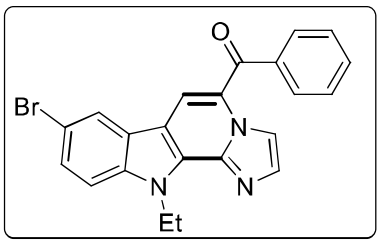

(35ga): Yellow solid (52 mg, 62%); m.p. 204-206 °C; ^{1}H NMR (400 MHz, Chloroform-*d*) δ 9.17 (s, 1H), 8.05 (s, 1H), 8.01 (s, 1H), 7.86 (d, *J* = 6.0 Hz, 3H), 7.70 (t, *J* = 7.3 Hz, 1H), 7.60 (t, *J* = 7.9 Hz, 3H), 7.47 (d, *J* = 8.7 Hz, 1H), 5.12 (q, *J* = 7.2 Hz, 2H), 1.60 (t, *J* = 7.2 Hz, 3H); ^{13}C{^{1}H} NMR (100 MHz, Chloroform-*d*) δ 189.8, 138.8, 138.2, 136.5, 132.8, 132.2, 130.8, 129.6, 128.6, 128.3, 125.8, 125.1, 122.7, 119.1, 116.5, 114.4, 112.2, 111.7, 40.5, 15.2; FT-IR ν_{max} (neat) 2350, 1627, 1504, 1242, 717 cm^{-1}; HRMS (ESI) calcd for $C_{22}H_{17}BrN_3O$ [M + H]$^{+}$: 418.0550, found 418.0562 and 420.0542.

Methyl 5-benzoyl-11-ethyl-11*H*-imidazo[1',2':1,2]pyrido[3,4-*b*]indole-9-carboxylate (35ha):

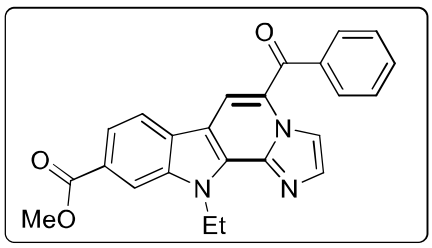

Yellow solid (81 mg, 94%); m.p. 234-236 °C; ^{1}H NMR (400 MHz, Chloroform-*d*) δ 9.16 (d, *J* = 1.4 Hz, 1H), 8.32 (s, 1H), 8.07 (s, 1H), 8.02 (d, *J* = 8.3 Hz, 1H), 7.96 (d, *J* = 8.3 Hz, 1H), 7.88 – 7.86 (m, 3H), 7.72 – 7.68 (m, 1H), 7.60 (t, *J* = 7.5 Hz, 2H), 5.19 (q, *J* = 7.2 Hz, 2H), 4.02 (s, 3H), 1.64 (t, *J* = 7.1 Hz, 3H); ^{13}C{^{1}H} NMR (100 MHz, Chloroform-*d*) δ 189.8, 167.4, 139.0, 138.7, 136.5, 133.0, 132.2, 132.1, 129.7, 128.6, 127.0, 128.0, 126.0, 122.3, 119.6, 119.3, 116.7, 112.5, 112.2, 52.3, 40.6, 15.4; FT-IR ν_{max} (neat) 2360, 1665, 1535, 1249, 730 cm^{-1}; HRMS (ESI) Calcd for $C_{24}H_{20}N_3O_3$ [M + H]$^{+}$: 398.1499, found 398.1516.

(11-Benzyl-11*H*-imidazo[1',2':1,2]pyrido[3,4-*b*]indol-5-yl)(phenyl)methanone (35ia): Yellow solid (39 mg, 46%); m.p. 190-192 °C; ^{1}H NMR (400 MHz, Chloroform-*d*) δ 9.20 (s, 1H), 8.12 (s, 1H), 7.99 – 7.81 (m, 4H), 7.70 – 7.68 (m, 1H), 7.63 – 7.59 (m, 2H), 7.50 – 7.41 (m, 2H), 7.37 – 7.25 (m, 6H), 6.42 (s, 2H); ^{13}C{^{1}H} NMR (100 MHz, Chloroform-*d*) δ 189.8, 140.0, 139.0, 137.1, 137.0, 132.7, 132.1, 131.0, 129.7, 128.8, 128.6, 127.6, 127.2, 125.8, 123.6, 121.6, 119.9, 119.4, 116.3, 113.3, 111.3, 48.9; FT-IR ν_{max} (neat) 2360, 1627, 1496, 1265, 694 cm^{-1}; HRMS (ESI) calcd for $C_{27}H_{20}N_3O$ [M + H]$^{+}$: 402.1601, found 402.1619.

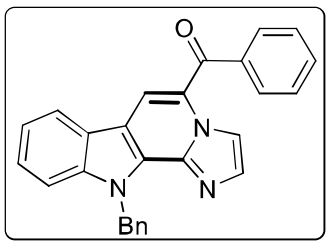

(11-Benzyl-8-methoxy-11*H*-imidazo[1',2':1,2]pyrido[3,4-*b*]indol-5-yl)(phenyl)methanone (35ja): Yellow solid (41 mg, 50%); m.p. 191-192 °C; ^{1}H NMR (400 MHz, Chloroform-*d*) δ 9.18 (s, 1H), 8.07 (s, 1H), 7.91 (d, *J* = 7.5 Hz, 2H), 7.82 (s, 1H), 7.70 (t, *J* = 7.3 Hz, 1H), 7.62 (t, *J* = 7.5 Hz, 2H), 7.35 (d, *J* = 8.9 Hz, 2H), 7.30 – 7.18 (m, 5H), 7.05 (dd, *J* = 8.9, 2.5 Hz, 1H), 6.38 (s, 2H), 3.89 (s, 3H); ^{13}C{^{1}H} NMR (100 MHz, Chloroform-*d*) δ 189.7, 155.6, 139.1, 137.2, 137.0, 134.9, 132.5, 132.0, 131.3, 129.7, 128.8, 128.6, 127.6, 127.1, 125.4, 124.3, 119.6, 116.2, 115.3, 113.0, 112.1, 102.2, 56.0, 49.0; FT-IR ν_{max} (neat) 2360, 1620, 1473, 1273, 756 cm^{-1}; HRMS (ESI) calcd for $C_{28}H_{22}N_3O_2$ [M + H]$^{+}$: 432.1707, found 432.1743.

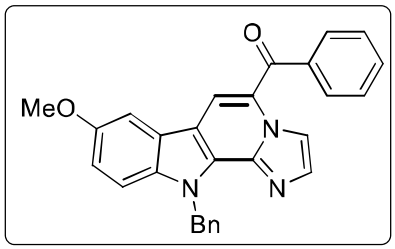

(11-Benzyl-8-bromo-11*H*-imidazo[1,2-*a*]indeno[2,1-*c*]pyridin-5-yl)(phenyl)methanone (35ka): Yellow solid (30 mg, 40%); m.p. 234-236 °C; ^{1}H NMR (400 MHz, Chloroform-*d*) δ 9.17 (d, *J* = 1.4 Hz, 1H), 8.04 (d, *J* = 1.9 Hz, 1H), 8.02 (s, 1H), 7.90 – 7.87 (m, 2H), 7.83 (d, *J* = 1.4 Hz, 1H), 7.73 – 7.69 (m, 1H), 7.62 (t, *J* = 7.5 Hz, 2H), 7.48 (dd, *J* = 8.7, 1.9 Hz, 1H), 7.33 (d, *J* = 8.7 Hz, 2H), 7.27 – 7.24 (m, 4H), 6.39 (s, 2H); ^{13}C{^{1}H} NMR (100 MHz, Chloroform-*d*) δ 189.8, 138.7, 138.6, 136.7, 132.9, 132.3, 131.4, 129.7, 128.8, 128.6, 128.5, 127.8, 127.1, 126.1, 125.3, 122.6, 119.0, 116.5, 114.8, 112.7, 112.2, 49.1; FT-IR ν_{max} (neat) 2380, 1610, 1425, 1230, 770 cm^{-1}; HRMS (ESI) calcd for $C_{27}H_{19}BrN_3O$ [M + H]$^{+}$: 480.0706; found 480.0703 and 482.0685.

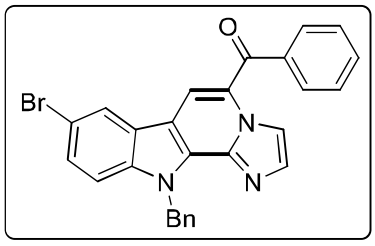

Methyl-benzoyl-11-benzyl-11*H*-imidazo[1',2':1,2]pyrido[3,4-*b*]indole-9-carboxylate (35la):

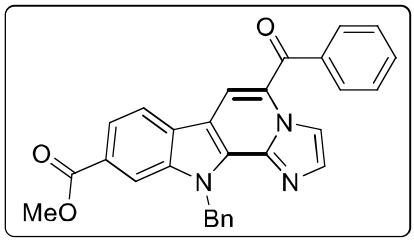

Yellow solid (38 mg, 49%); m.p. 228-230 °C; ^{1}H NMR (400 MHz, Chloroform-*d*) δ 9.16 (s, 1H), 8.24 (s, 1H), 8.09 (s, 1H), 7.97 (dd, *J* = 19.6, 8.4 Hz, 2H), 7.90 (d, *J* = 7.5 Hz, 2H), 7.85 (s, 1H), 7.71 (t, *J* = 7.4 Hz, 1H), 7.61 (t, *J* = 7.5 Hz, 2H), 7.35 – 7.27 (m, 5H), 6.45 (s, 2H), 3.97 (s, 3H); ^{13}C{^{1}H} NMR (100 MHz, Chloroform-*d*) δ 189.9, 167.2, 139.5, 138.7, 136.8, 136.7, 133.0, 132.5, 132.3, 129.7, 128.8, 128.6, 127.7, 127.2, 126.3, 122.6, 119.6, 119.2, 116.7, 113.0, 112.7, 52.3, 48.9; FT-IR ν_{max} (neat) 2360, 1670, 1430, 1250, 720 cm^{-1}; HRMS (ESI) calcd for $C_{29}H_{22}N_3O_3$ [M + H]$^{+}$: 460.1656, found 460.1650.

(11-Benzyl-2,3-diphenyl-11*H*-imidazo[1',2':1,2]pyrido[3,4-*b*]indol-5-yl)(phenyl)methanone

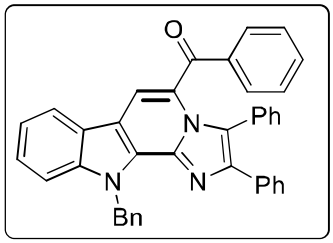

(35ij): Yellow solid (35 mg, 30%); m.p. 200-202 °C; ^{1}H NMR (400 MHz, Chloroform-*d*) δ 7.99 (d, *J* = 7.9 Hz, 1H), 7.75 (s, 1H), 7.64 (d, *J* = 7.1 Hz, 2H), 7.58 – 7.4 (m, 8H), 7.38 – 7.31 (m, 5H), 7.28 – 7.16 (m, 8H), 6.53 (s, 2H); ^{13}C{^{1}H} NMR (100 MHz, Chloroform-*d*) δ 188.2, 141.7, 140.1, 137.8, 137.0, 136.7, 134.5, 132.9, 131.7, 129.9, 129.2, 129.2, 128.7, 128.6, 128.4, 128.3, 128.2, 128.1, 127.7, 127.5, 127.3, 125.5, 124.2, 123.6, 121.8, 119.9, 113.7, 113.6, 111.1, 48.9; FT-IR ν_{max} (neat) 2360, 1635, 1257, 740 cm^{-1}; HRMS (ESI): Calculated $C_{39}H_{28}N_3O$ [M + H]$^{+}$: 554.2227, found 554.2242.

2-(1*H*-Imidazol-1-yl)-3-(1-methyl-1*H*-indol-3-yl)-1-phenylprop-2-en-1-one (36aa): Yellow

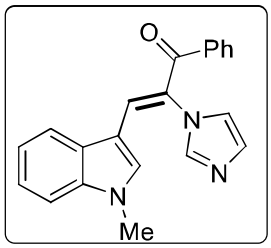

solid (95 mg, 93 %); m.p. 150-152 °C; ^{1}H NMR (400 MHz, Chloroform-*d*) δ 8.03 (s, 1H), 7.77 – 7.74 (m, 2H), 7.61 – 7.56 (m, 2H), 7.54 – 7.48 (m, 3H), 7.37 (s, 1H), 7.33 – 7.30 (m, 2H), 7.25 – 7.21 (m, 1H), 6.99 (s, 1H), 5.99 (s, 1H), 3.70 (s, 3H); ^{13}C{^{1}H} NMR (100 MHz, Chloroform-*d*) δ 191.2, 138.2, 136.8, 135.4, 132.3, 131.9, 130.4, 128.9, 128.4, 128.2, 127.7, 123.5, 121.9, 118.9, 118.2, 110.2, 107.7, 33.7; FT-IR ν_{max} (neat) 2370, 1610, 1512, 1257, 732 cm^{-1}; HRMS (ESI) calcd for $C_{21}H_{18}N_3O$ [M + H]$^{+}$: 328.1444, found 328.1444.

(7-Methyl-7*H*-imidazo[1',2':1,2]pyrido[4,3-*b*]indol-5-yl)(phenyl)methanone (38aa): Red solid (73 mg, 72%); m.p. 208-209 °C; ^{1}H NMR (400 MHz, Chloroform-*d*) δ 8.79 (d, *J* = 1.4 Hz, 1H), 8.66 (d, *J* = 7.9 Hz, 1H), 7.90 (d, *J* = 7.2, Hz, 2H), 7.82 (d, *J* = 1.5 Hz, 1H), 7.71 (t, *J* = 7.4 Hz, 1H), 7.60 (t, *J* = 7.6 Hz, 2H), 7.54 (t, *J* = 7.6 Hz, 1H), 7.47 – 7.46 (m, 1H), 7.42 – 7.39 (m, 2H), 3.82 (s, 3H); ^{13}C{^{1}H} NMR (100 MHz, Chloroform-*d*) δ 190.2, 142.4, 141.0, 138.1, 133.9, 132.8, 132.8, 129.9, 129.8, 128.7, 126.7, 123.4, 121.2, 121.0, 113.7, 111.0, 109.2, 108.9, 29.8; FT-IR ν_{max} (neat) 2360, 1635, 1535, 1249, 717 cm^{-1}; HRMS (ESI) calcd for $C_{21}H_{16}N_3O$ $[M + H]^+$: 326.1288; found 356.1295.

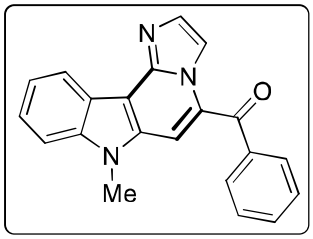

(7-Methyl-7*H*-imidazo[1',2':1,2]pyrido[4,3-*b*]indol-5-yl)(*p*-tolyl)methanone (38ab): Red solid (86 mg, 80%); m.p. 224-226 °C; ^{1}H NMR (400 MHz, Chloroform-*d*) δ 8.71 – 8.69 (m, 2H), 7.84 – 7.82 (m, 3H), 7.60 – 7.56 (m, 1H), 7.54 (s, 1H), 7.49 (d, *J* = 8.3 Hz, 1H), 7.46 – 7.42 (m, 1H), 7.40 (d, *J* = 7.9 Hz, 2H), 3.90 (s, 3H), 2.53 (s, 3H); ^{13}C{^{1}H} NMR (100 MHz, Chloroform-*d*) δ 190.0, 143.9, 142.5, 141.0, 135.2, 134.2, 132.7, 130.2, 129.4, 126.6, 123.5, 121.3, 121.2, 113.5, 110.8, 109.2, 108.3, 29.8, 21.8; FT-IR ν_{max} (neat) 2340, 1655, 1567, 1244, 730 cm^{-1}; HRMS (ESI) calcd for $C_{22}H_{18}N_3O$ $[M + H]^+$: 340.1444, found 340.1447.

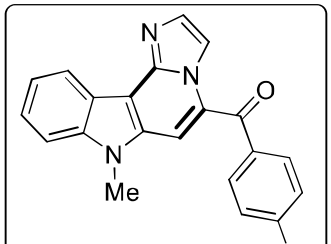

(7-Methyl-7*H*-imidazo[1',2':1,2]pyrido[4,3-*b*]indol-5-yl)(thiophen-2-yl)methanone (38ag): Red solid (85 mg, 82%); m.p. 172-174 °C; ^{1}H NMR (400 MHz, Chloroform-*d*) δ 8.66 (d, *J* = 7.9 Hz, 1H), 8.56 (d, *J* = 1.5 Hz, 1H), 7.85 (dd, *J* = 11.8, 4.1Hz, 2H), 7.80 (d, *J* = 1.5 Hz, 1H), 7.75 (s, 1H), 7.56 (t, *J* = 7.5 Hz, 1H), 7.47 (d, *J* = 8.3Hz, 1H), 7.43 (t, *J* = 7.5 Hz, 1H), 7.30 – 7.28 (m, 1H), 3.93 (s, 3H); ^{13}C{^{1}H} NMR (100 MHz, Chloroform-*d*) δ 181.5, 143.2, 142.4, 140.9, 135.0, 134.7, 134.2, 132.7, 130.0, 128.3, 126.6, 123.4, 121.2, 121.1, 113.2, 110.8, 109.2, 106.8, 29.9; FT-IR ν_{max} (neat) 2340, 1885, 1578, 1234, 788 cm^{-1}; HRMS (ESI) calcd for $C_{19}H_{14}N_3OS$ $[M + H]^+$: 332.0852, found 332.0856.

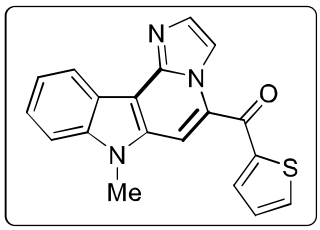

(7-Ethyl-7*H*-imidazo[1',2':1,2]pyrido[4,3-*b*]indol-5-yl)(phenyl)methanone (38ba): Red solid

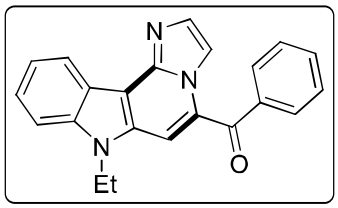

(72 mg, 74%); m.p. 237-238 °C; ^{1}H NMR (400 MHz, Chloroform-*d*) δ 9.40 (d, *J* = 8.1 Hz, 1H), 8.58 (s, 1H), 8.15 (d, *J* = 7.5 Hz, 2H), 7.98 (s, 1H), 7.83 (d, *J* = 6.3 Hz, 2H), 7.74 (t, *J* = 7.6 Hz, 2H), 7.63 – 7.56 (m, 1H), 7.53 (d, *J* = 8.2 Hz, 1H), 7.47 (t, *J* = 7.4 Hz, 1H), 4.62 (q, *J* = 7.3 Hz, 2H), 1.48 (t, *J* = 7.2 Hz, 3H); ^{13}C{^{1}H} NMR (100 MHz, Chloroform-*d*) δ 188.8, 140.2, 136.2, 136.1, 135.8, 134.4, 130.5, 129.3, 128.5, 128.4, 124.7, 123.4, 121.6, 119.2, 114.2, 110.9, 109.7, 105.7, 39.3, 14.7; FT-IR ν_{max} (neat) 1643, 1450, 1257, 1118, 948, 694 cm^{-1}; HRMS (ESI) calcd for $C_{22}H_{18}N_3O$ $[M + H]^+$: 340.1444, found 340.1452.

(7-Benzyl-7*H*-imidazo[1',2':1,2]pyrido[4,3-*b*]indol-5-yl)(phenyl)methanone (38ca): Red solid

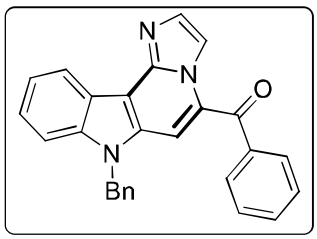

(34 mg, 40%), m.p. 205-207 °C; ^{1}H NMR (400 MHz, Chloroform-*d*) δ 8.88 – 8.71 (m, 2H), 7.89 – 7.84 (m, 1H), 7.69 – 7.64 (m, 3H), 7.52 – 7.46 (m, 5H), 7.38 – 7.35 (m, 1H), 7.29 – 7.26 (m, 3H), 7.00 (bs, 2H), 5.42 (s, 2H); ^{13}C NMR (100 MHz, Chloroform-*d*) δ 190.0, 142.4, 140.9, 137.8, 136.3, 133.5, 133.0, 132.6, 129.9, 129.4, 129.0, 128.5, 128.0, 126.9, 126.4, 123.6, 121.4, 121.3, 113.8, 111.7, 109.8, 109.5, 47.0; FT-IR ν_{max} (neat) 2379, 1663, 1564, 1230, 738 cm^{-1}; HRMS (ESI) calcd for $C_{27}H_{20}N_3O$ $[M+H]^+$: 402.1601, found 402.1600.

(7-Benzyl-7*H*-imidazo[1',2':1,2]pyrido[4,3-*b*]indol-5-yl)(naphthalen-2-yl)methanone (38cf):

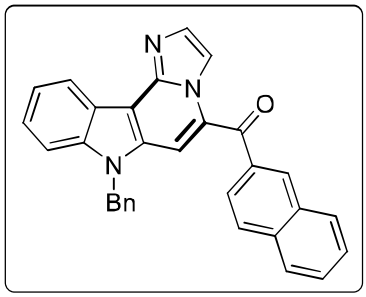

Red solid (50 mg, 52%); m.p. 232-234 °C; ^{1}H NMR (400 MHz, Chloroform-*d*) δ 8.83 (d, *J* = 1.4 Hz, 1H), 8.80 (d, *J* = 7.9 Hz, 1H), 8.20 (s, 1H), 7.97 (d, *J* = 8.5 Hz, 2H), 7.90 – 7.88 (m, 2H), 7.79 (d, *J* = 8.1 Hz, 1H), 7.69 (t, *J* = 7.5 Hz, 1H), 7.63 – 7.57 (m, 4H), 7.51 – 7.47 (m, 1H), 7.24 (t, *J* = 7.4 Hz, 3H), 7.00 (d, *J* = 7.5 Hz, 2H), 5.53 (s, 2H); ^{13}C{^{1}H} NMR (100 MHz, Chloroform-*d*) δ 189.7, 140.9, 135.9, 135.4, 132.1, 131.9, 129.9, 129.7, 129.1, 128.9, 128.8, 128.1, 127.9, 127.8, 127.4, 127.1, 126.3, 125.8, 125.5, 123.9, 122.1, 121.6, 121.3, 120.3, 119.9, 113.8, 109.6, 47.2; FT-IR ν_{max} (neat) 2330, 1636, 1574, 1296, 756 cm^{-1}; HRMS (ESI) calcd for $C_{31}H_{22}N_3O$ $[M+H]^+$: 452.1757, found : 452.1756.

(7-Benzyl-7*H*-imidazo[1',2':1,2]pyrido[4,3-*b*]indol-5-yl)(thiophen-2-yl)methanone (38cg):

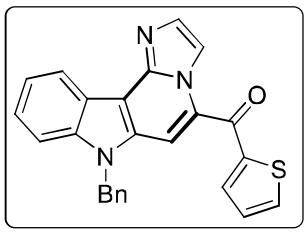

Red solid (37 mg, 43%); m.p. 185-187 °C; ^{1}H NMR (400 MHz, Chloroform-*d*) δ 8.77 (d, *J* = 8.0 Hz, 1H), 8.60 (s, 1H), 7.83 – 7.79 (m, 2H), 7.68-7.47 (m, 5H), 7.34-7.32 (m, 3H), 7.11 (bs, 3H), 5.64 (s, 2H); ^{13}C{^{1}H} NMR (100 MHz, Chloroform-*d*) δ 182.1, 176.6, 138.4, 137.6, 136.1, 131.7, 130.2, 129.9, 129.0, 128.0, 125.0, 124.4, 123.4, 123.3, 122.1, 121.7, 118.9, 116.8, 116.7, 108.5, 104.7, 102.9, 42.5; FT-IR ν_{max} (neat) 2386, 1679, 1522, 1255, 713 cm^{-1}; HRMS (ESI) calcd for $C_{25}H_{18}N_3OS$ $[M+H]^+$: 408.1165, found 408.1207.

(5-Benzyl-5*H*-benzo[4',5']imidazo[1',2':1,2]pyrido[4,3-*b*]indol-7-yl)(phenyl)methanone

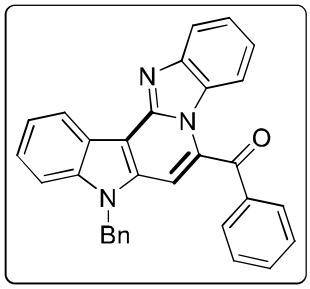

(38ck): Red solid (22 mg, 23%); m.p. 217-219 °C; ^{1}H NMR (400 MHz, Chloroform-*d*) δ 8.90 (s, 1H), 8.11 (d, *J* = 8.2 Hz, 1H), 8.03 (d, *J* = 7.8 Hz, 2H), 7.73 (t, *J* = 7.5 Hz, 1H), 7.56 – 7.49 (m, 7H), 7.29 – 7.28 (m, 4H), 7.23 – 7.19 (m, 1H), 7.09 – 7.07 (m, 2H), 5.61 (s, 2H); ^{13}C{^{1}H} NMR (100 MHz, Chloroform-*d*) δ 189.0, 139.9, 135.9, 135.7, 134.7, 134.3, 130.7, 129.1, 129.0, 128.5, 128.0, 126.3, 126.2, 125.1, 123.4, 122.1, 122.1, 120.9, 114.2, 109.8, 103.4, 47.4; FT-IR ν_{max} (neat) 2377, 1675, 1530, 1260, 715 cm^{-1}; HRMS (ESI) calcd for $C_{31}H_{22}N_3O$ $[M + H]^+$: 452.1757, found 452.1750.

Imidazo[1,2-*a*]thieno[3,2-*c*]pyridin-5-yl(phenyl)methanone (40aa): Red solid (47 mg, 38%);

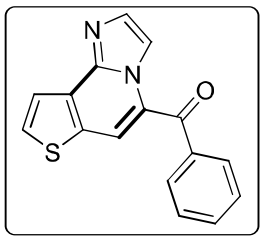

m.p. 195-193 °C; ^{1}H NMR (400 MHz, Chloroform-*d*) δ 8.82 (s, 1H), 8.07 (d, *J* = 5.3 Hz, 1H), 7.88 – 7.86 (m, 1H), 7.85 (d, *J* = 1.5 Hz, 1H), 7.83 (d, *J* = 4.9 Hz, 1H), 7.79 (bs, 1H), 7.76 (bs, 1H), 7.70 – 7.66 (m, 1H), 7.59 – 7.55 (m, 2H); ^{13}C{^{1}H} NMR (100 MHz, Chloroform-*d*) δ 190.1, 142.5, 137.6, 132.9, 132.9, 132.5, 132.4, 131.8, 129.8, 129.1, 128.7, 122.8, 118.3, 115.3; FT-IR ν_{max} (neat) 2345, 1655, 1540, 1260, 711 cm^{-1}; HRMS (ESI) calcd for $C_{16}H_{11}N_2OS$ $[M+H]^+$: 279.0587; found 279.0585.

Imidazo[1,2-*a*]thieno[3,2-*c*]pyridin-5-yl(4-methoxyphenyl)methanone (40ac): Red solid (57 mg, 42%); m.p. 200-202 °C; ^{1}H NMR (400 MHz, Chloroform-*d*) δ 8.61 (s, 1H), 8.08 (s, 1H), 7.90 (d, *J* = 8.3 Hz, 2H), 7.82 – 7.72 (m, 3H), 7.06 (d, *J* = 8.4 Hz, 2H), 3.95 (s, 3H); ^{13}C{^{1}H} NMR (100 MHz, Chloroform-*d*) δ 188.7, 163.9, 142.4, 133.3, 132.4, 132.0, 131.7, 131.1, 129.8, 129.5, 122.8, 116.6, 115.0, 114.1, 55.7; FT-IR ν_{max} (neat) 2330, 1671, 1587, 1274, 713 cm^{-1}; HRMS (ESI) calcd for $C_{17}H_{13}N_2O_2S$ [M + H]$^{+}$: 309.0692; found 309.0685.

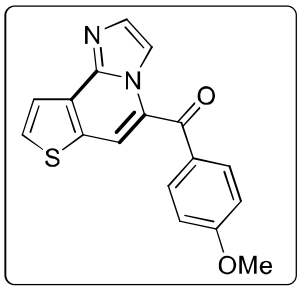

Benzofuro[2,3-*c*]imidazo[1,2-*a*]pyridin-5-yl(phenyl)methanone (42): Yellow solid (34 mg, 32%); m.p. 170-171 °C; ^{1}H NMR (400 MHz, Chloroform-*d*) δ 8.90 (d, *J* = 1.6 Hz, 1H), 8.75 (d, *J* = 7.6 Hz, 1H), 7.94 – 7.90 (m, 3H), 7.80 (s, 1H), 7.74 (d, *J* = 7.4 Hz, 1H), 7.72 – 7.68 (m, 2H), 7.64 – 7.63 (m, 1H), 7.62 – 7.58 (m, 2H); ^{13}C{^{1}H} NMR (100 MHz, Chloroform-*d*) δ 189.6, 157.3, 151.2, 140.4, 137.1, 133.4, 132.3, 130.7, 129.9, 128.8, 124.8, 124.0, 121.6, 114.9, 114.6, 111.8, 110.5; FT-IR ν_{max} (neat) 2353, 1651, 1550, 1249, 1134, 1010, 725 cm^{-1}; HRMS (ESI) calcd for $C_{20}H_{13}N_3O_2$ [M + H]$^{+}$: 313.0972, found 313.0973.

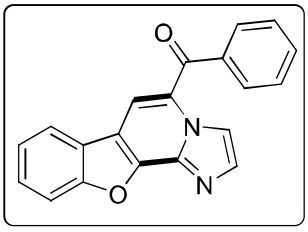

3-(1*H*-Indol-3-yl)-2-(2-(4-methoxyphenyl)-1*H*-imidazol-1-yl)-1-phenylprop-2-en-1-one (44): Pale red solid (14 mg, 10 %); m.p. 150-152 °C; ^{1}H NMR (400 MHz, Chloroform-*d*) δ 8.18 (s, 1H), 7.80 (d, *J* = 8.6 Hz, 2H), 7.76 (d, *J* = 4.6 Hz, 1H), 7.65 – 7.59 (m, 3H), 7.56 (d, *J* = 7.9 Hz, 1H), 7.54 – 7.48 (m, 2H), 7.44 – 7.40 (m, 2H), 7.33 (dd, *J* = 8.0, 1.9 Hz, 1H), 7.11 (s, 1H), 6.95 (d, *J* = 8.4 Hz, 2H), 6.63 (s, 1H), 3.86 (s, 3H), 3.81 (s, 3H); ^{13}C{^{1}H} NMR (100 MHz, Chloroform-*d*) δ 189.4, 162.7, 145.6, 137.1, 137.0, 136.6, 134.4, 132.6, 132.4, 130.3, 128.7, 128.7, 128.0, 126.1, 124.4, 123.8, 122.8, 122.0, 118.2, 114.9, 110.7, 107.4, 55.5, 29.7; FT-IR ν_{max} (neat) 2370, 1610, 1512, 1257, 732 cm^{-1}; HRMS (ESI) calcd for $C_{28}H_{24}N_3O_2$ [M + H]$^{+}$: 434.1863, found 434.1862.

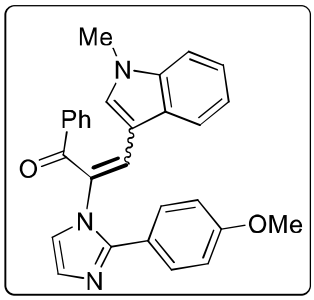

2.4.3 X-ray Crystallographic Analysis of Compound 35ha and 36aa

The single crystals of the compound **35ha** ($C_{24}H_{19}N_3O_3$) and compound **36aa** ($C_{21}H_{17}N_3O$) were obtained as greenish yellow and yellow crystal blocks respectively from ethyl acetate solutions. The crystal data collection and data reduction were performed using CrysAlis PRO on a single crystal Rigaku Oxford XtaLab Pro diffractometer. The crystal was kept at 93(2) K during data collection. Using Olex2[35], the structure was solved with the ShelXT[36] structure solution program using Intrinsic Phasing and refined with the ShelXL[37] refinement package using Least Squares minimization.

Table 2.5: Crystal data and structure refinement for **35ha.**

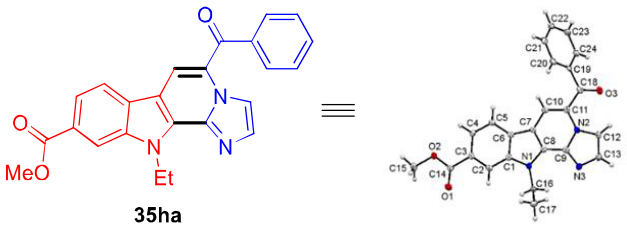

Identification code	exp_159_VNS176	ρ_{calc}g/cm^3	1.421
Empirical formula	$C_{24}H_{19}N_3O_3$	μ/mm^{-1}	0.096
Formula weight	397.42	F(000)	832.0
Temperature/K	93(2)	Crystal size/mm^3	0.3 × 0.2 × 0.1
Crystal system	monoclinic	Radiation	MoKα (λ = 0.71073)
Space group	$P2_1/n$	2Θ range for data collection/°	10.078 to 49.992
a/Å	9.4056(12)	Index ranges	-11 ≤ h ≤ 9, -8 ≤ k ≤ 8, -31 ≤ l ≤ 33
b/Å	7.0317(8)	Reflections collected	10670
c/Å	28.179(3)	Independent reflections	3247 [R_{int} = 0.0183, R_{sigma} = 0.0205]
α/°	90	Data/restraints/parameters	3247/0/273
β/°	94.395(10)	Goodness-of-fit on F^2	1.039
γ/°	90	Final R indexes [I>=2σ (I)]	R_1 = 0.0324, wR_2 = 0.0821
Volume/Å^3	1858.2(4)	Final R indexes [all data]	R_1 = 0.0407, wR_2 = 0.0862
Z	4	Largest diff. peak/hole/eÅ^{-3}	0.18/-0.20

Table 2.6: Crystal data and structure refinement for **36aa.**

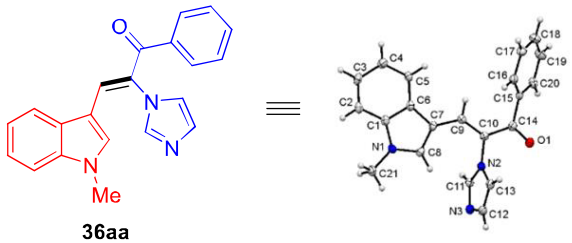

36aa

Identification code	exp_164-vns139	ρ_{calc}g/cm^3	1.298
Empirical formula	$C_{21}H_{17}N_3O$	μ/mm^{-1}	0.082
Formula weight	327.38	F(000)	344.0
Temperature/K	93(2)	Crystal size/mm^3	0.2 × 0.1 × 0.1
Crystal system	monoclinic	Radiation	MoKα (λ = 0.71073)
Space group	$P2_1$	2Θ range for data collection/°	10.332 to 49.994
a/Å	8.8630(6)	Index ranges	$-10 \leq h \leq 10$, $-8 \leq k \leq 7$, $-14 \leq l \leq 16$
b/Å	6.9410(4)	Reflections collected	5002
c/Å	14.0380(10)	Independent reflections	2563 [R_{int} = 0.0401, R_{sigma} = 0.0447]
α/°	90	Data/restraints/parameters	2563/1/227
β/°	104.114(7)	Goodness-of-fit on F^2	1.067
γ/°	90	Final R indexes [I>=2σ (I)]	R_1 = 0.0311, wR_2 = 0.0821
Volume/Å^3	837.52(10)	Final R indexes [all data]	R_1 = 0.0346, wR_2 = 0.0838
Z	2	Largest diff. peak/hole/eÅ^{-3}	0.13/-0.14

2.5 REFERENCES

1. Parsons, P. J.; Penkett, C. S.; Shell, A. J., *Chemical Reviews* **1996,** *96*, 195-206.
2. Shul'pin, G. B., *Dalton Transactions* **2013,** *42*, 12794-12818.
3. Pandey, K.; Rangan, K.; Kumar, A., *The Journal of Organic Chemistry* **2018,** *83*, 8026-8035.
4. Nandwana, N. K.; Shinde, V. N.; Saini, H. K.; Kumar, A., *European Journal of Organic Chemistry* **2017,** *2017*, 6445-6449.
5. Nicolaou, K.; Montagnon, T.; Snyder, S. A., *Chemical Communications* **2003**, 551-564.
6. Lu, L. Q.; Chen, J. R.; Xiao, W. J., *Accounts of Chemical Research* **2012,** *45*, 1278-1293.

7. Wender, P. A., *Tetrahedron* **2013,** *69*, 7529-7550.
8. Wang, Z.; Li, K.; Zhao, D.; Lan, J.; You, J., *Angewandte Chemie International Edition* **2011,** *50*, 5365-5369.
9. Liu, C.; Yuan, J.; Gao, M.; Tang, S.; Li, W.; Shi, R.; Lei, A., *Chemical Reviews* **2015,** *115*, 12138-12204.
10. Liu, C.; Zhang, H.; Shi, W.; Lei, A., *Chemical Reviews* **2011,** *111*, 1780-1824.
11. Suzuki, A., *Angewandte Chemie International Edition* **2011,** *50*, 6722-6737.
12. Yang, Y.; Lan, J.; You, J., *Chemical Reviews* **2017,** *117*, 8787-8863.
13. Gao, D. W.; Gu, Q.; You, S. L., *Journal of the American Chemical Society* **2016,** *138*, 2544-2547.
14. Ashenhurst, J. A., *Chemical Society Reviews* **2010,** *39*, 540-548.
15. Liégault, B.; Lee, D.; Huestis, M. P.; Stuart, D. R.; Fagnou, K., *The Journal of Organic Chemistry* **2008,** *73*, 5022-5028.
16. Sridharan, V.; Martin, M. A.; Menendez, J. C., *European Journal of Organic Chemistry* **2009,** *2009*, 4614-4621.
17. Gandeepan, P.; Hung, C.-H.; Cheng, C. H., *Chemical Communications* **2012,** *48*, 9379-9381.
18. Laha, J. K.; Jethava, K. P.; Dayal, N., *The Journal of Organic Chemistry* **2014,** *79*, 8010-8019.
19. Laha, J. K.; Dayal, N.; Jethava, K. P.; Prajapati, D. V., *Organic Letters* **2015,** *17*, 1296-1299.
20. Ackermann, L.; Jeyachandran, R.; Potukuchi, H. K.; Novak, P.; Büttner, L., *Organic Letters* **2010,** *12*, 2056-2059.
21. Sun, M.; Wu, H.; Zheng, J.; Bao, W., *Advanced Synthesis & Catalysis* **2012,** *354*, 835-838.
22. Reddy, V. P.; Iwasaki, T.; Kambe, N., *Organic & Biomolecular Chemistry* **2013,** *11*, 2249-2253.
23. Saito, K.; Chikkade, P. K.; Kanai, M.; Kuninobu, Y., *Chemistry–A European Journal* **2015,** *21*, 8365-8368.
24. Pintori, D. G.; Greaney, M. F., *Journal of the American Chemical Society* **2011,** *133*, 1209-1211.

25. Tripathi, K. N.; Ray, D.; Singh, R. P., *Organic & Biomolecular Chemistry* **2017,** *15*, 10082-10086.
26. Tripathi, K. N.; Bansode, A. H.; Singh, R. P., *Synthesis* **2020,** *52*, 719-726.
27. Ray, D.; Manikandan, T.; Roy, A.; Tripathi, K. N.; Singh, R. P., *Chemical Communications* **2015,** *51*, 7065-7068.
28. Tripathi, K. N.; Ray, D.; Singh, R. P., *European Journal of Organic Chemistry* **2017,** *2017*, 5809-5813.
29. Mantenuto, S.; Ciccolini, C.; Lucarini, S.; Piersanti, G.; Favi, G.; Mantellini, F., *Organic Letters* **2017,** *19*, 608-611.
30. Zhu, W.; Tong, S.; Zhu, J.; Wang, M. X., *The Journal of Organic Chemistry* **2019,** *84*, 2870-2878.
31. Laha, J. K.; Sharma, S., *ACS Omega* **2018,** *3*, 4860-4870.
32. Gu, C. X.; Liu, J. G.; Chen, W. W.; Xu, M. H., *Tetrahedron* **2021,** *85*, 132048.
33. Sahoo, S.; Pal, S., *The Journal of Organic Chemistry* **2021,** *86*, 4081-4097.
34. Liu, C.; Shi, C.; Mao, F.; Xu, Y.; Liu, J.; Wei, B.; Zhu, J.; Xiang, M.; Li, J., *Molecules* **2014,** *19*, 15653-15672.
35. Dolomanov, O. V.; Bourhis, L. J.; Gildea, R. J.; Howard, J. A.; Puschmann, H., *Journal of Applied Crystallography* **2009,** *42*, 339-341.
36. Sebbar, N.; Ellouz, M.; Essassi, E.; Ouzidan, Y.; Mague, J., *Acta Crystallographica Section E: Crystallographic Communications* **2015,** *71*, o999.
37. Sheldrick, G. M., *Acta Crystallographica Section A: Foundations and Advances* **2015,** *71*, 3-8.